



**Politecnico  
di Torino**

**Politecnico di Torino**

Corso di Laurea

A.a. 2021/2022

Sessione di Laurea Marzo 2022

**Nanomedicine for Drug Delivery:  
Design of nano-formulations to  
improve transport anti-cancer  
drugs**

Relatori:

Prof. Ciardelli Gianluca

Prof.ssa Mattu Clara

Prof. Tuszynski Jacek Adam

Candidati:

Renna Antonio

## Contents

<b>1</b>	<b>Introduzione .....</b>	<b>3</b>
1.1	Nanomedicine in cancer treatment: general concepts .....	4
1.1.1	Passive targeting .....	4
1.1.2	Active targeting .....	5
1.1.3	Stimuli-mediated tumor targeting .....	6
1.2	Classification of nanoformulations .....	6
1.3	Preparation techniques for polymer nanoparticles .....	8
1.3.1	Emulsion-based methods .....	8
1.3.2	Solvent displacement method (Nanoprecipitation) .....	9
1.3.3	Salting out method .....	9
1.3.4	Ionic crosslinking method .....	10
1.4	Physical and Chemical characterization of nanoparticles .....	11
<b>2</b>	<b>Microtubules.....</b>	<b>11</b>
2.1	MECHANISM OF POLYMERIZATION .....	13
2.2	Dinamic instability .....	13
<b>3</b>	<b>Tubulin Binding Agents.....</b>	<b>14</b>
3.1	Tubulin Binding Agents as antivasular strategies against cancer .....	14
3.2	Mechanism of resistance .....	15
3.3	ATP Binding Cassette .....	16
3.4	Glutathione detoxification system modificare la scrittura.....	16
3.5	$\alpha$ and $\beta$ tubulin.....	17
3.6	Colchicine .....	18
3.7	Structure .....	18
3.8	Tubuline and colchicine .....	19
3.9	Mechanisms of action of colchicine.....	19
1.1	Metabolism and toxicities .....	20
3.10	Interaction binding pocket of colchicine.....	20
3.11	CCI-001 .....	20
<b>4</b>	<b>Aim of the work.....</b>	<b>22</b>
<b>5</b>	<b>Materials and methods .....</b>	<b>22</b>
5.1	Materials.....	22
5.1.1	Chemicals and cell lines.....	22
5.2	Methods.....	23
5.2.1	Nanoparticles Preparation .....	23
5.2.2	Cellular tests.....	27
<b>6</b>	<b>Result and Discussion .....</b>	<b>28</b>
6.1	Nanoparticles Characterization .....	28
6.2	Hydrophobic NPs formulation .....	31
6.3	Drug release .....	32
6.4	Cellular tests.....	33
6.4.1	Response of the cells to free CCI-001.....	34
6.4.2	Tests on spheroids.....	35
<b>7</b>	<b>Conclusions .....</b>	<b>37</b>

**List of Figures**

Figure 1:Enhanced permeability and retention effect[13].....5  
 Figure 2:Active targeting[3] .....6  
 Figure 3:Double emulsion.....9  
 Figure 4:Schetatic illustration of the Nanoprecipitation method .....9  
 Figure 5:illustration scheme of salting out method.....10  
 Figure 6:: Ionic crosslinking method .....11  
 Figure 7:Structure of microtubules .....12  
 Figure 8:Microtubule polymerization and depolymerization mechanism [56] .....13  
 Figure 9: Microtubule binding sites overview .....15  
 Figure 10: Structure of colchicine.....19  
 Figure 11:main differences between Colchicine and CCI-001 .....21  
 Figure 1:Hydrophobic NPs synthesis protocol loaded with CCI-001.....24  
 Figure 2:Hydrophilic nanoparticle preparation method.....25  
 Figure 3:Hydrophilic NPs synthesis protocol with the phluorophore .....26  
 Figure 4: Size of NPs with 50,25 and 10% CF in the polymeric solution before and after centrifugation and picking up the supernatant. ....29  
 Figure 5: Size distribution for different CF percentage in the polymeric solution: a)50% CF formulation; b)25% CF formulation; c) 10 % CF formulation .....29  
 Figure 6: NPs size with 10% and 1% chloroform in polymer solution.....30  
 Figure 7:Hydrophobic NPs size with and without CCI-001 encapsulated.....31  
 Figure 8: DLS Size distribution for n=3 samples of: a)empty NPs; b) NPs with 50ug of CCI-001 in formulation; c) NPs with 100ug of CCI-001 in formulation .....32  
 Figure 9:Release of CCI-001 in water .....33  
 Figure 10: cultured U87 cells.....33  
 Figure 11:Cell viability of the cell exposed to free CCI-001 at various concentration at 24 and 48 h .....34  
 Figure 12:Cell viability 48 hours after exposure to different concentrations of :free CCI-001, empty NPs and encapsulated CCI-001 .....34  
 Figure 13:Images acquired in bright field microscopy for U87 cells treated with different concentration of free CCI-001, empty NPs and CCI-001 encapsulated in NPs observed at 48h.....35  
 Figure 14: U87 Cells spheroids after 4 days in culture .....35  
 Figure 15: Cell viability of the spheroid treated with empty NPs,free CCI-001 and CCI-001 encapsulated in the NPs observed at 24 hours .....36  
 Figure 16:Cell viability of the spheroid treated with empty NPs,free CCI-001 and CCI-001 encapsulated in the NPs observed at 48 hours .....36  
 Figure 17: Images acquired in bright field microscopy for U87 spheroids treated with different concentration of free CCI-001, empty NPs and CCI-001 encapsulated in NPs observed at 48h.....37

**1 Introduzione**

Nanomedicine is the application of Nanotechnologies to the design of nano-dimensioned drug carriers for treatment, diagnosis, and imaging of pathologies. Paul

Ehrlich introduced the concept of Nanomedicine: in 1910, when he was the first to hypothesize that it was possible to produce selective with a specific high chemical affinity towards a certain target and minimized side effects on the other organs. He called them *magic bullets*[1]. In 1959 Richard Feynman first spoke of the potential of Nanotechnology, by envisioning the possibility to manipulate the matter at the nanoscale, with his seminal talk *there's plenty of room at the bottom*. [2]

Since then, many advancements in Nanotechnology and Nanomedicine have been achieved, although only a few nano-formulations have been approved for clinical applications. For instance, in 1995 Doxil, the first nanodrug, was commercialized in US. Doxil is a liposomal formulation of doxorubicin and received approval for the treatment of Kaposi's sarcoma[4]. In 2005 Abraxane, an Albumin-bound paclitaxel nanoparticle was approved by FDA for the treatment of Metastatic breast cancer, in 2009 MEPACT, a Liposomal mifamurtide formulation was approved by the EMA for the treatment of treatment for osteosarcoma[3].

The low number of approved nano-formulations highlights the need for better tools to test and validate nanomedicines before they progress to clinical trials. Such tools should consider and reproduce the many biological barriers in the human body, that may be responsible for the clinical failure of nanomedicines, such as the immune system, the interstitial fluid pressure in tumors, and the vascular barrier, to name a few [5]. In addition, it is of paramount importance to adopt the correct selection of nanoparticles design methods and materials, to maximize drug encapsulation, reduce side effects and enhance the therapeutic efficacy of the nano formulations[6]

## **1.1 Nanomedicine in cancer treatment: general concepts**

As mentioned above, cancer nanotherapeutics are being implemented in medicine to solve the limitations of conventional Drug Delivery systems such as: nonspecific biodistribution, scarce targeting, poor oral bioavailability, and low therapeutic index[7]. The main advantage of nanoparticles in cancer treatment is the possibility to target specifically tumour cells and to protect drugs from biodegradation or excretion before reaching the target[8]. Generally speaking, nanoparticles can target tumors through two main strategies: passive and active targeting[9].

### **1.1.1 Passive targeting**

Passive targeting is based on the small size of nanoparticles[10] and was first reported by Maeda and co-workers[11]. They showed enhanced accumulation of long-circulating macromolecules in tumors, by extravasation through their more fenestrated and disorganized vessels. Indeed, due to the fast development and aggressive angiogenesis, the blood vessels irrigating certain tumors are more permeable with thinner and fenestrated walls. Moreover, tumors lack an efficient lymphatic drainage, which causes retention of substances[12]. Thus, nanoparticles of appropriate size can passively leak through the defective vascular endothelium of tumors and remain trapped. This feature of tumors was named the Enhanced Permeability and Retention effect (EPR), as shown in Figure 1 [13]

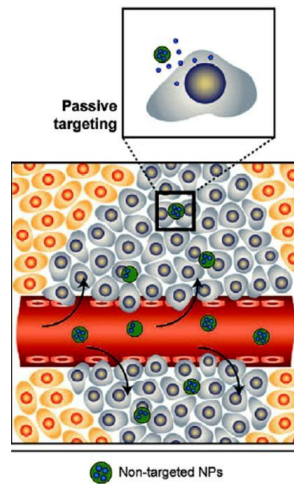


Figure 1: Enhanced permeability and retention effect[13]

### 1.1.2 Active targeting

Active targeting exploits a specific recognition of cancer cells by NP through receptor-ligand recognition[13]. Active targeting requires a close interaction between nanoparticles and the target cells, thus it is fundamental that the carriers are brought in the vicinity of the tumor, for example through passive targeting[14]. In addition, active targeting requires the surface-modification of nanoparticles with specific ligands able to interact with the target cancer cells.

Several cancer cells exhibit receptor over-expression compared to their normal counterparts, allowing their specific targeting[15]. By modifying the surface of nanoparticles with target-specific ligands, we can increase the specificity of tumor targeting by reducing the nonspecific release of the drug toward normal cells, and therefore, its side effects[16]. Active targeting strategies are limited by the heterogeneity of the tumor microenvironment, in which tumor cells may exhibit different level and type of mutations[17]. Thus, a too high specificity may only act on one part of the complex micro-environment of the tumour, leaving room for the other actors involved[18]. In Figure 2 is showed a schematization of Active Targeting

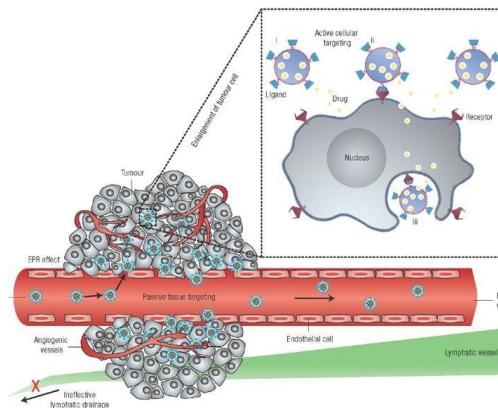


Figure 2:Active targeting()

### 1.1.3 Stimuli-mediated tumor targeting

In addition to the traditional concepts of active and passive targeting, nanoparticles can also be directed to the tumor by the application of an external stimulus or by exploiting tumor-specific stimuli, such as pH variations[19]. Nanoparticles that are designed to respond to specific stimuli, are also called smart nanomedicines[20].

This is also one of the most difficult and complex way to engineer a nanoparticle. The theoretical advantage of using a stimuli-responsive system is to release the drug only when needed and requested, thus minimizing systemic exposure to the compound[21].

## 1.2 Classification of nanoformulations

Typically, nanoformulations (nanoparticles) possess at least a characteristic size in the range between 1 and 400 nm. At the nanoscale, two primary factors influence the properties of materials:

- surface effects, due to highest surface/volume ratio, which results in properties scaling due to the higher fraction of atoms on the surface.
- quantum effects, due to quantum confinement materials with delocalized electrons.

These factors affect the chemical reactivity of materials, as well as their mechanical, optical, electric, and magnetic properties[22]. The small size of nanoparticles is especially advantageous in medicine because nanoparticles can not only circulate widely throughout the body but also enter cells or be designed to bind to specific cells.

Nanoparticles for drug delivery can be further classified according to their size, shape, and composition[3]. A general classification divides nanoparticles into:

- *Massive nanoparticles*: these are polymeric or inorganic nanocarriers in which the drug is finely dispersed into a dense matrix.[22][23]
- *Nanocapsules*: Typically, polymer or lipid-based hollow structures, in which a shell made of the selected material hosts the drug inside an inner cavity. In some instance (e.g., in the case of nano capsules made of lipid bilayers) the drug can also be dispersed in the shell.[24] [25]
- *Nanocomplexes*: which exploit electrostatic interactions, between the particle material (typically a polymer containing charged functional groups) and the drug of opposite charge. The most typical example is the encapsulation of nucleic acids, such as RNAs or DNA, into positively charged polymers, such as chitosan. [26]

Depending on the material they are composed of nanoparticles can also be divided into:

*Lipid based nanocarriers*. Depending on the choice of lipids, these can be liposomes, with at least one phospholipid bilayer that forms a hollow sphere or can be also massive solid lipid nanoparticle[25]. One example of these carriers is Doxil, a PEGylated liposomal doxorubicin formulation, that increased the therapeutic index of Doxorubicin by reducing its non-specific uptake, resulting in extended circulation time and higher tumour uptake[4].

*Inorganic nanoparticles*: for example, iron oxide or gold nanoparticles; silicon oxide nanoparticles, or quantum dots[27], mostly used for imaging and diagnosis rather than for drug delivery. For instance, iron oxide nanoparticles are used as MRI contrast agents[28]. Iron oxide and gold nanoparticles, if irradiated, can generate heat and are therefore exploited for hyperthermal tumor treatment[29]. Silica nanoparticles have been exploited for drug delivery, by entrapping drugs into their controlled nanoporous structures[30].

*Polymer based nanocarriers*: these are typically massive nanoparticles, with properties dependent on the material[31]. One example of polymer carrier is NAB-Paclitaxel, a particle obtained with the NAB (nanoparticle albumin bound) method, where the drug is bound to albumin, creating a protein-drug conjugate which self assembles into a nanoparticle, the drug is a *microtubule* stabilizer, that inhibits mitosis in cancer cells that undergo apoptotic-like cell death[33]. Depending on the polymer used and on its affinity toward the drug to be encapsulated, nanoparticles can encapsulate both, hydrophobic and hydrophilic, drugs. Typically, polymer nanoparticles are biocompatible and biodegradable, and their surface can be easily modified with functional group useful for further targeting[34]. Typical biopolymers used for nanoparticles preparation may be of synthetic or natural origin [35]. Synthetic biopolymers have attracted attention because of their stability, flexibility, low immunogenicity, and biodegradability. Table 1 summarizes the most used class of biopolymers used for the design of polymer nanoparticles.

Polymer class	Advantages	Disadvantages
Polyesters	Slow degradation for a[36] more controlled release	not soluble in water, need organic (usually toxic) solvents [37], limited to hydrophobic drugs.
Polyethers	Soluble in water. Some, such as PEG show antifouling and long-circulation properties[38][39].	Fast degradation by oxidation, uncontrolled release0.
Polyelectrolites	Natural polymers, such as chitosan or alginate, suitable for proteins and sensitive biomolecules, no need of surfactants[41].	Limited to water soluble drugs, pH sensitivity, limited choice of polymers, aggregation phenomena possible[42].
Polyurethanes	Tunable properties depending on the building blocks, suitable for both hydrophobic and hydrophilic drugs.[43]	Toxic solvent used in syntesis[44]

Table 1: Main polymer-based nanoparticles summary

### 1.3 Preparation techniques for polymer nanoparticles

Depending on the polymer selection, different preparation techniques can be selected, as described below.

#### 1.3.1 Emulsion-based methods

Emulsions are formed using two immiscible phases and mechanical mixing in presence of surfactants, which contribute to the formation of droplets of one phase incorporating the other (typically, the phase present in larger quantity[45]). The surfactants are amphiphilic molecules that stabilize the droplets and localize at the interface between the two phases. Emulsions can be classified as oil in water (o/w) when the water predominates or water in oil(w/o) if vice versa, considering oil an organic solvent immiscible in water. The most used solvent are dichloromethane, tetrahydrofuran, and ethyl acetate, with the latter showing a low toxicity profile[46]. The most widely used polymers with this method are degradable polyesters, such as PCL, PLA, and PLGA. Typically, solvent evaporation requires an increase of temperature and/or pressure, which may destabilize the particles or damage the encapsulated drug. Once the solvent is evaporated, the nanoparticles and the drugs tend to solidify, being not soluble in water, and the residues of solvent and surfactant are removed by repeated centrifugation. This method is quite easy to scale-up, with NP size regulated by concentration of the surfactant and by the intensity of mixing. The main difficulties rely in the removal of residual surfactant, toxicity of the solvents, and incompatibility with the water-soluble drugs.

To encapsulate water soluble drugs, double emulsions can be used, such as the water in oil in water (w/o/w) emulsion[47]. Here, the primary emulsion is water in oil, where the water solution contains the drug and the oil phase contains the solution of polymer in the organic solvent, the water phase is dispersed in the oil phase, forming droplets entrapping the hydrophilic drug. This primary emulsion is then added to the secondary water solution, containing the surfactant to form a secondary emulsion. In this way, the solvent, which is not water-soluble, forms droplets containing the previous droplets of water/solvent/drug. Figure 3 shows an example of both the type of Double emulsions.

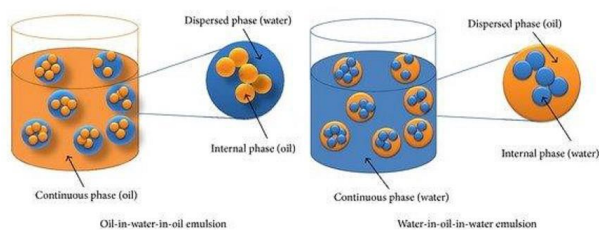


Figure 3: Double emulsion

### 1.3.2 Solvent displacement method (Nanoprecipitation)

This method uses two phases, as shown in figure 4: the solvent phase, miscible with water (e.g., acetone or acetonitrile) and a non-solvent (water). The polymer and the drug are soluble in the solvent but not in water[48]. The polymer is dissolved in the organic solvent and added dropwise to a solution of water containing the surfactant, under mechanical stirring. In this way, nanoparticles are rapidly formed for the fast diffusion (displacement) of the solvent from the polymeric core of the particles towards the aqueous phase, followed by collection and washing of nanoparticles by repeated centrifugation steps. The NPs obtained by this method are monodispersed and relatively tiny (200 nm). Moreover, the method uses non-toxic solvents and easily removable surfactants, but is only indicated for hydrophobic drugs and is hard to scale-up.

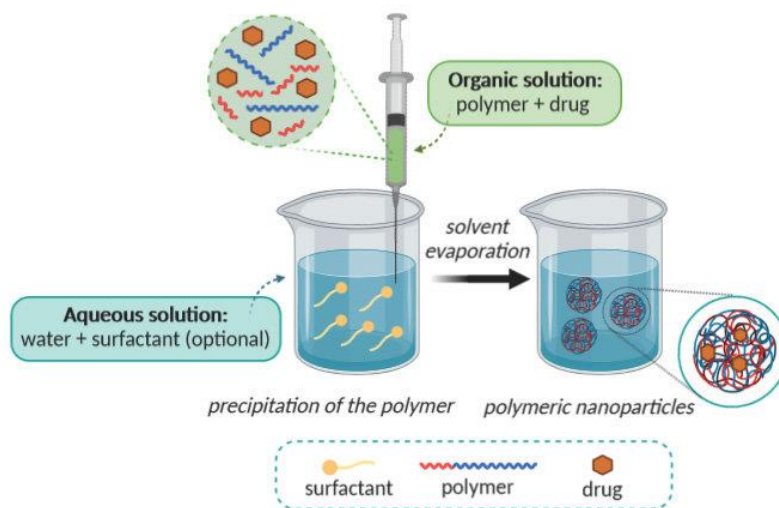


Figure 4: Schematic illustration of the Nanoprecipitation method

### 1.3.3 Salting out method

This method (Figure 5) uses two solvents (one of which is water), which are miscible under specific conditions. The water phase contains an electrolyte, the salting-out agent (usually  $\text{CaCl}_2$  or  $\text{MgCl}_2$ ) that reduces the miscibility with the solvent. The organic solvent contains the polymer and the drug, making only hydrophobic drug suitable for

the method. The organic solvent is added in water containing the salting out agent and emulsified. Once the emulsion is formed, water is added to the system altering the concentration of the electrolyte and restoring the possibility for the solvent to diffuse in water. The main advantage is to limit the action of pressure and temperature to evaporate the solvent as in traditional emulsion-based methods[49].

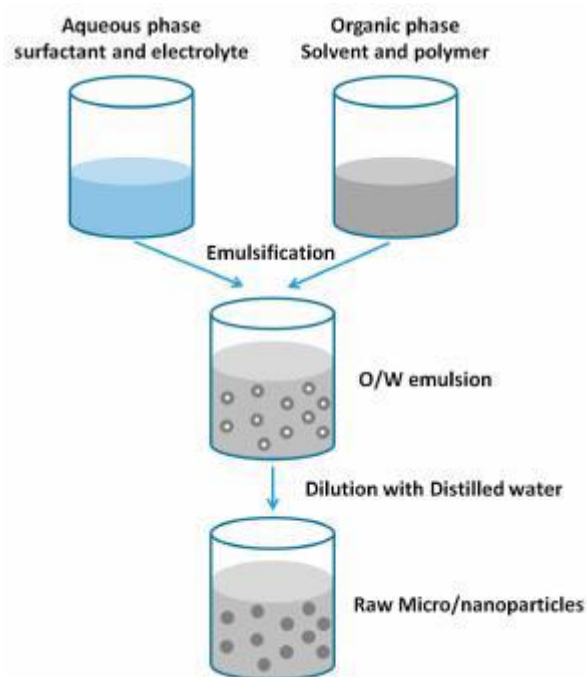


Figure 5: illustration scheme of salting out method

#### 1.3.4 Ionic crosslinking method

This method relies on mild agitation to form particles in water stabilized by a crosslinking agent and exploits polymers with charged groups, such as chitosan or alginate, and a cross-linking agent of opposite charge (Figure 6). The method requires only water as a solvent and is thus suitable only for hydrophilic drugs and water-soluble polymers. Surfactants are not needed and the bioactivity of the molecules to be encapsulates is well preserved. The nanoparticles assume a gel-like state with a pseudo spherical shape.

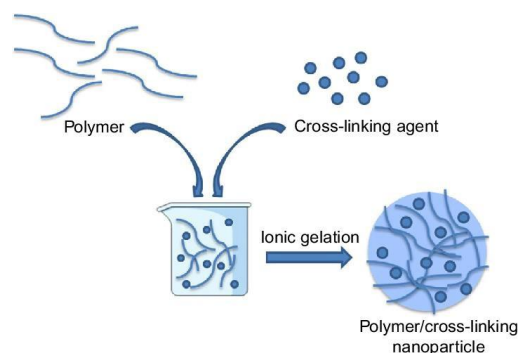


Figure 6: Ionic crosslinking method

#### 1.4 Physical and Chemical characterization of nanoparticles

The main features of nanoparticles are structure, composition, size, surface properties, charge, and stability[50]. Typically, the size distribution of nanoparticles is determined by measuring their hydrodynamic size and polydispersity index (PDI), which is a measure of the heterogeneity of particles' size distribution.

The surface charge of the nanoparticles is another important parameter to determine and is typically evaluated through  $\zeta$ -potential measurements. The  $\zeta$  potential allows to predict the aggregation behaviour of nanoparticles in suspension. Typically, values ranging from 0 to  $\pm 5$  indicate rapid coagulation or flocculation, values from  $\pm 10$  to  $\pm 40$  indicate incipient to modest stability, while values from  $\pm 40$  to  $\pm 60$  indicate good stability[51].

## 2 Microtubules

Microtubules are an ubiquitous cytoskeletal structure that are formed by the self assembly of the tubulin heterodimer. Microtubules are involved in diverse functions like cell motility, form and morphogenesis, intracellular vesicle transport, chromosome segregation during mitosis, and due to this ubiquity are an auspicious target for many novel treatment. Numerous ligands binds to tubulin, affecting its assembling properties, and among them several drugs have proven to have anticancer properties. Microtubules are assembled into rigid hollow rods with internal diameter of 12 nm and external diameter of 25 nm that can achieve 50  $\mu\text{g}$  of length, composed of a set of 13 parallel protofilament of tubulin heterodimer. These dynamic structures that can undergo unstopped assembly and disassembly within cell. [56] Tubulin is a dimer consisting of two 55 kDa

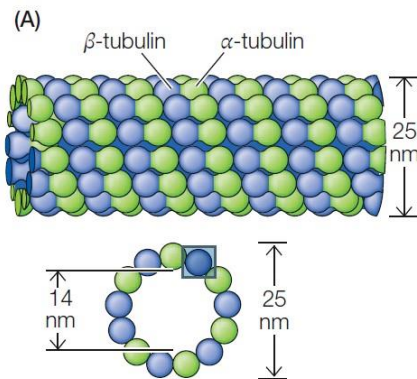


Figure 7: Structure of microtubules

polypeptides called  $\alpha$  and  $\beta$  tubulin, homologous dimers with about 40% identical sequence, each monomer composed by a core of two  $\beta$ -sheets surrounded by a helix. A third type of tubulin,  $\gamma$ -tubulin, found in the centrosome, has a fundamental role in initiating the microtubule assembly. Microtubules have univocal dimers orientation that gives them polarity:  $\alpha$  faces are the slow growing minus end,  $\beta$  ones the fast growing plus end involved in the microtubule assembly. Polarity, in a similar way of actin filaments, is important in order to determine the direction of movement along microtubules. Each monomer

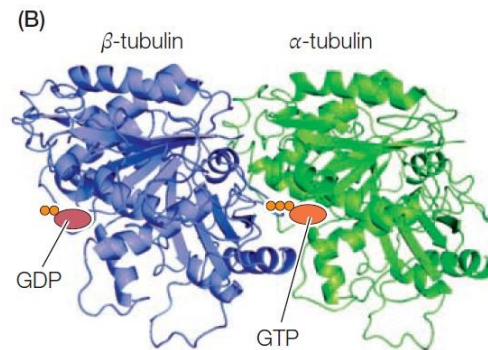


Figure 2: structure of a tubulin dimer with GTP bound to  $\alpha$ -tubulin and GDP bound to  $\beta$ -tubulin [56]

has 3 functional domains: amino-terminal domain, nucleotide binding region, made by six parallel  $\beta$ -strands alternating with 6 loops, with another helix completing the binding site. 3 ulterior helices and  $\beta$ -strand form a taxol binding domain. Two anti-parallel helices represent the carboxy-terminal domain, the protein binding site. The  $\gamma$ -tubulin forms a ring structure that contain from 10 to 13  $\gamma$ -tubulin localized in the centrosome, serves to initiate microtubule assembly starting from the minus ends.

## 2.1 MECHANISM OF POLYMERIZATION

Both  $\alpha$  and  $\beta$ -tubulin bind to GTP, in order to regulate polymerization, with the GTP bound to  $\beta$ -tubulin hydrolyzed to GDP during or shortly after polymerization. The GTP hydrolysis weakens the tubulin affinity to bind to the adjacent molecule of tubulin, hence favoring depolymerization at the minus end. There are two main mechanisms of polymerization of the microtubules:

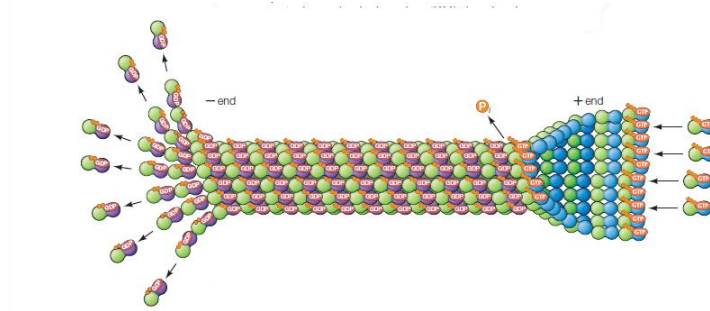


Figure 8: Microtubule polymerization and depolymerization mechanism [56]

- Treadmilling: A dynamic behavior of microtubules in which occurs the loss of subunits with GDP bound lost from the minus end of the filament balanced by their addition to the other end, binding to GTP-containing tubulin;
- Dynamic instability: A mechanism powered by bonding of to GTP at the microtubule plus end in the elongation phase, whereas  $\beta$ -tubulin bound to GDP by hydrolysis stops assembling (MT loss of the cap), lowering the affinity of tubulin with nearby molecules, alternating in this way cycles of growth and shrinkage.

## 2.2 Dynamic instability

Microtubules grow by binding of GTP-tubulin subunits. After they are incorporated into the microtubule,  $\beta$ -subunits are hydrolyzed to GDP-tubulin, weakening the binding affinity of tubulin with the nearby molecules. GDP-tubulin is most stable in a curved state. Once microtubule shrinkage begins, by loss of the GTP-tubulin cap at the end, the GDP-tubulin is free to spread out and the microtubule rapidly shrinks. Dynamic instability plays an essential role in mitosis, through the formation of the mitotic spindle, so the Mt are used as therapeutic targets to prevent cellular division, that is one of the key functions to treat tumours.

Growth or shortening phase is according to GTP-Bound Tubulin molecular ratio, so if addition rate prevails over hydrolysis MT is in growth phase and viceversa. [57] The prevalence of growing or shortening of the MT divide the dynamic instability in 4 sub-phases:

- Growing phase
- Shortening Phase
- Catastrophic phase: transition from growth to shortening or pause phase
- Rescue phase: transition from shortening to growth or pause phase

Microtubules do not function alone; they interact with an array of microtubule-associated proteins (MAPs) that influence their assembly and dynamics. Microtubules features and functions are determined by the tubulin code , a combination of tubulin isotypes and post-translational modifications of tubulin (PTMs). Both  $\alpha$ - and  $\beta$ -tubulin can be modified by phosphorylation, acetylation, palmitoylation, removal and subsequent addition of carboxy-terminal tyrosines, and addition of multiple glutamines or glycines. Different isotypes in microtubules can have two main functions: first, it could affect the primary structure of tubulin dimers and therefore physical properties, dynamic instability of MT and its interaction with the MAPs.

### **3 Tubulin Binding Agents**

Tubulin-binding drugs can be classified according to the site on tubulin where they bind to or according to the mechanism through which they inhibit polymerization of MT. Most of these agents target the taxane-binding site, which are stabilizer. These include the taxanes, the epothilones, discodermolide, eleutherobin and launilamide. The other two sites currently targeted therapeutically are destabilizer, vice versa, bind to tubulin leading to a curved conformation of tubulin from a straight one, accounted for the loss of lateral contacts between protofilaments, characteristic of rings or depolymerizing microtubules: the Vinca binding site, by agents including the cryptophycin analogues, dolastatins, maytansinoid immunoconjugates, viniflunine and halichondrin B analogues, and the colchicine-binding site, by agents such as Colchicine Combretastatin A4 and its analogues. Drugs that bind to the colchicine domain have been reported to show promising as vascular-targeting agents even if for some agents, the precise binding site has not been fully characterised. Finally, the microtubule can also be targeted by a number of novel agents that do not directly target tubulin, such as therapeutics targeting the microtubule-associated proteins (MAP) and the immunoconjugates. [58]

#### **3.1 Tubulin Binding Agents as antivasular strategies against cancer**

One of the many TBA strategies against cancer are the anti vascular strategies, cause the vasculature is easily accessible to blood-borne therapeutic agents, and tumour cells die rapidly unless they are supplied by oxygen and nutrient by the blood. Two main antivasular strategies were developed for cancer treatment, by using the angiogenic inhibitors, inhibiting the formation of new blood vessels (AIs) by targeting the pro-angiogenic signaling pathways and the ligand receptor systems or the vascular disrupting agents (VDAs), that target and rapidly shut down the existing tumour vasculature, impairing the endothelial cytoskeleton morphology and vascular permeability. VDAs: Vascular disrupting agents Small molecule VDAs include flavonoids and tubulin-binding agents (TBAs). Flavonoids cause actin cytoskeleton derangements in endothelial cells, stimulating cell death. TBAs bind to different sites of tubulin and they operate

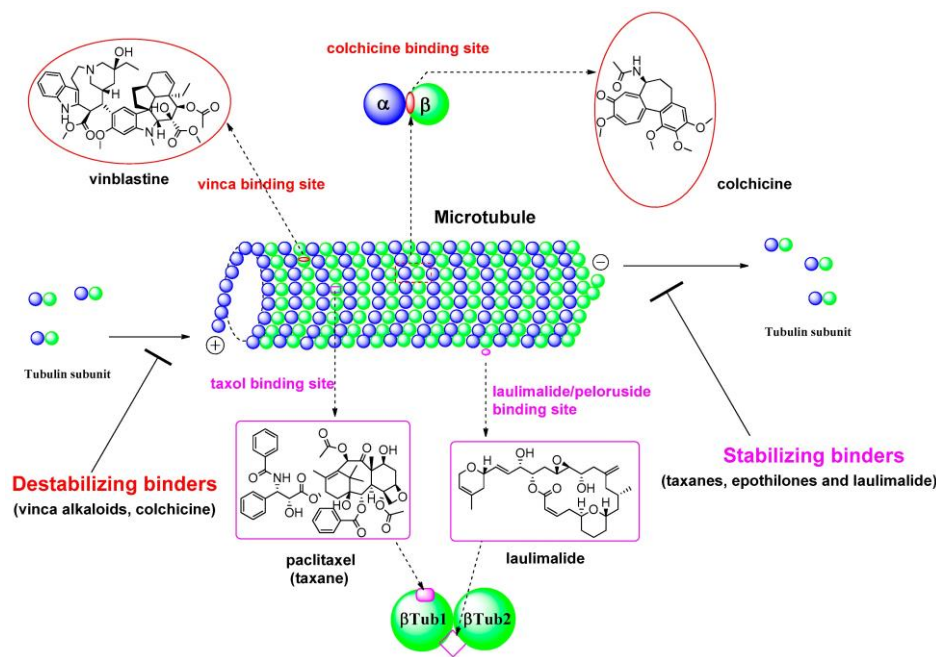


Figure 9: Microtubule binding sites overview

as microtubule-stabilizing or destabilizing agents. TBAs have shown higher efficacy than flavonoids. They were originally used as antimetotics in cancer, but they are endowed also with antivascular activity. Most of them are CA-4 derivatives, that resemble colchicine and bind to the colchicine binding site and they were tested both as single agents and in combination with chemotherapeutic drugs. The obtained results are promising, but single treatments led to insufficient clinical benefits. The more effective approaches are based on combination treatments, focused on the inhibition of both tumor mass and its vasculature. The use of multiple pharmacological strategies may overcome the resistance mechanisms induced by the tumor microenvironment. Combination therapy results in the better strategy to eradicate the entire tumor, but the adequate dosing and scheduling need to be further investigated [59].

### 3.2 Mechanism of resistance

Cancer cells possess different mechanisms of resistance to TBAs, there are two main types of resistance that cells have against anticancer drugs: the intrinsic one, is the resistance before the cancer cells get exposure to anticancer compound, and it may be caused by several factors as tumor microenvironment and/or genetic mutation. The acquired resistance is generated by high exposure to cytotoxic drugs. Most investigated mechanisms of resistance with clinical significance are:

- activation of transmembrane proteins effluxing the chemical compounds in and out of the cells (ABC transporters)
- activation of the enzymes of glutathione detoxification system;

- alteration of the genes and the proteins involved into the modulation of apoptosis
- mutation and overexpression of specific tubulin isotypes

### 3.3 ATP Binding Cassette

Some cancer cells don't respond properly to microtubule-binding agents(MBA), often due to the fact that several of the pathways previously analysed, can lead to multidrug resistance (MDR), in which cell are resistant to several drugs in addition to the initial compound, MDR cells also display usually other properties, such as genome instability and loss of checkpoint control, that complicates therapy, ABC genes play an important role in MDR[60]. The ATP binding cassette (ABC) modulates the flux of substances and represents the main mechanism of resistance, and use the energy produced by the hydrolysis. ABCs are transmembrane regulatory proteins, whose overexpression, associated to gene amplification, epigenetic and transcriptional changes, can lead to multi drug resistance in cancer(MDR)[61], in which cancer cells transport different anticancer compounds, catalyzing the ATP-dependent transport across cellular membrane especially for the most in people with defected ABC genes[62]. ABC are composed by two domains, the Nucleotide Binding Domain (NBD) and the Trans Membrane Domain (TMD). The TMD spans the membrane, producing channels determining the properties of the transported substrates. One of the most famous ABC transporters is the 170 kDa P-glycoprotein ( P-gp) belonging to the ABCB family, that is proven to interact with more than 200 compounds. It possess a large flexible drug-binding pocket characterized by low specificity, that can be exploited to develop inhibitors and modulator, blocking its transport function[63]. The P-gp can be inhibited in three ways: first, by blocking the drug binding site, secondly by interfering with ATP hydrolysis and the third by altering cell membrane lipids and their integrity[64].

### 3.4 Glutathione detoxification system modificare la scrittura

Another mechanism involved in multi-drug resistance (MDR) is constituted by glutathione and its associated enzymes like glutathione S-transferases (GST) that have been widely investigated and seems to be linked to the existence of a MDR in cancer cells[65],it recognizes various chemical compounds and mediates their transports in and out of the cells, having the fundamental role to protect the cells: GSH is the most abundant antioxidant found in living organisms. When GSH binds to a compound, it has the capability to make that compound less toxic and more hydrophilic, which imply that it makes more easy to be cleared from the body. Metabolism of drugs is composed of two main phases:

- phase I, where P-450 isozyme family makes small changes to the drugs phase I, by producing reactive sites which can covalently interact with other molecules;
- phase II, cytoprotective, where GST isozyme family makes the drugs more hydrophilic and less toxic.[66]

In cells,metabolic processes such as respiration and oxidative stress are linked to the formation of reactive oxygen species (ROS)[67], those can be very harmful to cells and also they may be associated with DNA damage that leads to different diseases, dysfunctions and ageing processes. Glutathione may provide defence not only against

ROS, but also against their toxic products. ROS production is dramatically higher in cancer cells because of the particular microenvironment characteristics, such as mitochondrial dysfunction, genetic mutations and abnormal metabolism[68].

GSH and ROS play a dual role, having both a tumour promoting and a tumour suppressing functions[69]: moderate ROS levels can stimulate survival and proliferation of tumour cells by activating signaling pathways that help the cancer to grow in stressful environment. High levels of ROS, which are often found in cancer, can cause damage to the cells, provoking cell death. Tumours, have the necessity to modulate ROS and antioxidants, therefore, elevated levels of GSH are involved in the protection of tumour cells. The complexes formed by GSH-GST-drug obtained are effluxed out of the cell through multiple resistance associated protein transporters (MRP1). Tumours are often characterized by high levels of GST and MRP1 [68].

### 3.5 $\alpha$ and $\beta$ tubulin

$\alpha$  and  $\beta$  tubulin dimers are highly homologous. Each monomer binds to a guanine nucleotide, which is non exchangeable in  $\alpha$  tubulin, and is exchangeable in  $\beta$  tubulin in E-site. GTP at the E-site is required for microtubule assembly, its hydrolysis follows addition of a dimer to the microtubule end, upon which becomes non-exchangeable[70]. The major interest in  $\beta$ -tubulin is due also because is the most diffuse and the less conservative monomer. Most of the drugs that target tubulin bind tubulin indiscriminately to the  $\beta$  subunit, leading to death of both healthy and tumour cells,  $\beta$ -tubulin have several isotypic forms and different diffusion among different tissues. There appears to exist 9 different isotypes in humans [71][72]. Of these isotypes, distinguished by Carboxy terminal tail,  $\beta$ Ia,  $\beta$ IVb and  $4\beta$  are almost ubiquitous in normal tissues and hence would be poor anti-tumor drug targets.  $\beta$ Ib and  $\beta$ IVa have much narrower distributions but are too similar to  $\beta$ Ia and  $\beta$ IVb, respectively, to imagine a drug able to be specific for either of them. Indeed  $\beta$ Ia,  $\beta$ Ib,  $\beta$ IVa and  $\beta$ IVb closely resemble each other. In contrast,  $\beta$ II, which differs significantly from these four, is elevated in many tumors, with relatively restricted distribution in normal tissues of all the isotypes.  $\beta$ III is less abundant in brain than  $\beta$ II, and seems to be the most promising target for drug development, with distribution in normal tissues restricted to testis and neurons, and is over expressed in many tumors, particularly in those aggressive, metastatic and drug resistant, having a protective effect in tumor cells, especially against oxidative stress, and also increase sensibility to drugs as docetaxel and taxol, and trastuzumab, and seems to target only neurons and not glia, reducing the potential damage to the nervous tissue and its survival[73].  $\beta$ III more diffused in tumor tissue  $\beta$ III in normal cells are more expressed in Brain neurons, but not involving the glia cells, fundamental for the survival of neuronal cells, and are also involved in the endothelial blood vasculature tissue, whereas in tumoral field are overexpressed in cells with a strong resistance against taxanes; brain tumor cells, lung tumor cells, pancreatic adenocarcinoma; renal carcinoma and malignant melanoma[74].  $\beta$ III are also a suitable tumoral marker[75], cause its overexpression is bound to:

- hypoxic condition and a altered expression of HIF1 $\alpha$  ;
- oxidative stress condition ruled by interaction between  $\beta$ III and glutathion S transferase

- metabolic stress ruled by  $\beta$ II and its implication in glucose response
- autophagy activity linked, with metabolic stress influenced by TBA, suppressor of the MT dynamics
- interrupting cell death signaling
- more aggressive breast, prostate and colorectal cancer
- invasive tumors compared to non invasive.[74]

All factors involved in the survival of the tumoral environment. Suppressing  $\beta$ III and targeting its connected mechanism could make tumor cells more vulnerable to chemotherapy.

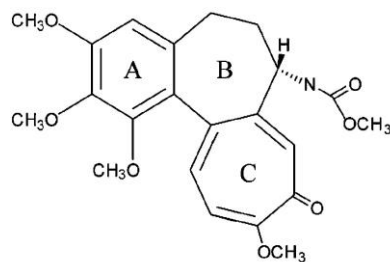
### 3.6 Colchicine

Colchicine is a very ancient drug known from about 3000 years ago, a major alkaloid first isolated in 1820, from *Colchicum autumnale* and *gloriosa superba*. Its molecular weight is 399.44. its brute formula is  $C_{22}H_{25}NO_6$ .

Colchicine is considered first-line therapy for treatment of acute gout, prophylaxis of gout, and familial Mediterranean fever. It is also commonly used in other diseases including pseudogout, pericarditis, Behçet's disease and neutrophilic dermatoses. Colchicine interacts mainly with tubulin, cytochrome P3A4 (CYP3A4) and P-glycoprotein[76], a transmembrane protein associated with multi drug resistance, that makes the currently available chemotherapy ineffective and increase of the expression of  $\beta$ III tubulin isotype.[77]

### 3.7 Structure

The determination of colchicine's structure required decades, although in 1945, Michael Dewar made an important contribution when he suggested that, among the molecule's three rings, two were seven-member rings. The ring A is trimethoxy benzene ring, B is a seven membered ring with an acetoamido group located at its C7 position, and ring C a methoxy tropone ring. the 1-methoxy group is important to setting the correct conformation of the molecule[78], whereas the trimethoxyphenyl group has important role in binding ability, cause replacing it with bulky groups results in great reduction of the tubulin affinity[79] Ring B is also crucial for colchicine tubuline interaction cause can easily undergo photochemical decomposition and resulting in reduced binding ability [80].



**COL**

*Figure 10: Structure of colchicine.*

### 3.8 Tubuline and colchicine

Colchicine blocks cell division by disrupting microtubules. It binds to soluble tubulin leading to the formation of a tubulin-colchicine complex (TC-complex). This complex then undergoes co-polymerization into microtubule end with the majority of the tubulins being unaffected. The microtubule ends have the ability to polymerize further, but TC-complexes induce a conformation change, which prevents the microtubules growth by sterically blocking further addition of the tubulin dimers at the ends. It is known as the “end conserving mechanism”, which suggests the TC-complex doesn’t completely prevent the tubulin addition but only slows new tubulin addition. Colchicine depolymerizes microtubules at high concentration and arrests microtubule growth at low concentration[81]

### 3.9 Mechanisms of action of colchicine

Colchicine binds to free tubulin dimers which, when incorporated into nascent microtubules, disrupt further microtubule polymerization, inhibiting vesicle transport, cytokine secretion, phagocytosis, migration and division, interfering so with a lot of phases of the cellular cycle. At higher concentrations colchicine may also induce some microtubule dissociation[82]. Colchicine is also an antimetabolic drug which blocks mitotic cells in metaphase. It binds to soluble tubulin to form tubulin-colchicine complexes in a poorly reversible manner, binding to the ends of the microtubules to prevent the elongation of the microtubule polymer. Colchicine has a concentration dependent behaviour: at low concentration arrests microtubule growth, at higher promotes microtubule depolymerisation[83]. It also inhibits cancer cell migration and metastatic potential, inhibits angiogenesis[84], also could favor apoptotic cell death through limitation of ATP influx into mitochondria. It also has anti-inflammatory effects, mainly related to disruption of microtubules, interfering with neutrophil adhesion and recruitment to inflamed tissue, also inhibiting neutrophil extravasation during inflammation, therefore reducing oxidative stress by reducing calcium influx into neutrophils.

## 1.1 Metabolism and toxicities

Colchicine has a narrow therapeutic window, the most common adverse reaction when prescribed for familial mediterranean fever are abdominal pain, diarrhoea, nausea, and vomiting, but in a mild transient and reversible way upon lowering the dose. prescribed for gout flares the most common adverse reaction is diarrhoea. Colchicine doses of 0.5 to 0.8 mg/kg are highly toxic, and doses of more than 0.8 mg/kg are typically lethal [82] Colchicine is a substrate for intestinal and hepatic cytochrome P450 3A4 (CYP3A4), and also a substrate for P-glycoprotein 1 (P-gp) reflux transporter. current colchicine metabolism understandings states certain drugs could increase potential toxicity via modulation of P-gp and CYP3A4 activity, in fact are reported fatal drug interaction with concomitant P-gp inhibitor and strong CYP3A4 inhibitors [76].

## 3.10 Interaction binding pocket of colchicine

In 2004, Ravelli et al. identified the colchicine-binding site at the interface of the  $\alpha$ - $\beta$  tubulin heterodimer. While the binding site for colchicine is located between the  $\alpha$  and  $\beta$  tubulin monomers, the principal interaction zone is dislocated on the  $\beta$  subunit. The colchicine-binding pocket was identified within the intermediate domain of  $\beta$  tubulin [85].

Colchicine and its analogues have also showed potential in inhibit cancer cell proliferation through colchicine binding site to microtubules dissociating them into tubulin dimers and acting as antimetabolic agents, and promoting the research of less toxic derivatives of thiocolcoside and colchicine [77].

Colchicine is primarily eliminated by hepatobiliary excretion in patient with normal renal function. P-gp is encoded by the multidrug resistance gene-1 a modulation of the P-gp and cyp could induce a better excretion [76]. It causes severe toxicity to normal tissue at high dose, limiting therefore its use in cancer therapy.

In addition, colchicine inhibits neutrophil superoxide anion production and increases leukocyte cAMP, which is known to suppress neutrophil function. At low concentrations (e.g., 3 nM), colchicine modulates inhibiting neutrophil adhesion to, and extravasation from the vasculature. At higher concentrations (e.g., 300 nM), further impeding neutrophil-endothelial cell adhesion. These concentration-dependent effects may partly explain the observation that low doses (e.g., 0.6 mg/day) of colchicine may prevent, but doses higher (e.g., 1.8 mg) are needed to suppress acute gouty attacks. Other potential anti-inflammatory activities include modulation of pyrin expression (see familial Mediterranean fever section), downregulation of lipopolysaccharide-induced TNF- $\alpha$  mRNA production, inhibition of histamine release by mast cells, suppression of pro-collagen synthesis, and promotion of collagenase activity [86].

## 3.11 CCI-001

Colchicine derivative were developed to overcome P-gp efflux in order to reduce the typical multi drug resistance of the cells over expressing  $\beta$ -III in presence of the colchicine. Colchicine interacts with P-gp by hydrophobic bounds, enhancing, via conformational changes the efflux of colchicine and other drugs. Most of the better known anti cancer drugs fails to bind to cell over expressing  $\beta$ -III tubulin, so silencing it would make easier to bind other drugs, as like Paclitaxel, doxorubicin and cisplatin.

The structure of CCI-001 has been modified to increase the  $\beta$ -III tubulin affinity, that differs from the colchicine for thiomethyl at c-10 position, methyl carbamate at c-7 position and for the acetate group at c-3. The  $\beta$ -III tubulin affinity has been verified through derivative binding affinity. Predicted binding free energies (kcal/mol) with respect to major tubulin

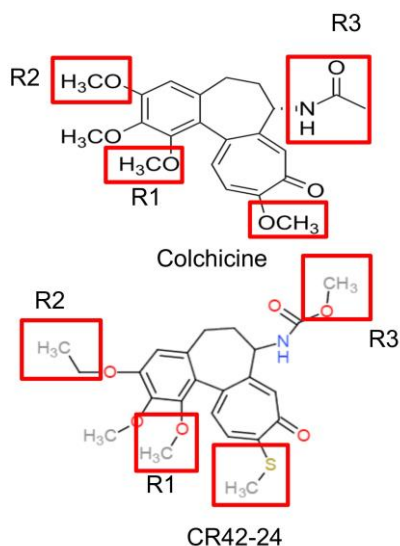


Figure 11: main differences between Colchicine and CCI-001

isotypes:  $\beta$ I: -53.1;  $\beta$ IIa: -34.4;  $\beta$ IIb: -39.1;  $\beta$ III: -48.4;  $\beta$ IVa: -32.0;  $\beta$ IVb: -44.0;  $\beta$ V: -63.8;  $\beta$ VI: -47.6.

After finding the compound as one of the most promising were conducted evaluation of the effects on microtubules using A549 cells and using as negative control untreated cells, and as positive control colchicine at concentration of 1  $\mu$ M for two hours as for the compound in exam here. It resulted in blebbing, disorganized cytoskeleton and membrane damage. The half minimal inhibitory concentration, IC<sub>50</sub> resulted 100-1000 lower than colchicine, therefore resulting more suitable for a release controlled by little doses comparable to those of nanoparticles. Solubility at pH 7.4 result 0.007 mg/mL, making this compound suitable for Hydrophobic nanocapsule compounds.

Toxicity studies evidenced reducing a lot of side effects resulting in parent compound, with the more acute resulted now only in intestinal irritation with test on rats.

Other test to evaluate the Cytotoxicity on A549, NCI-H226, and CEM cell lines showed Cytotoxicity with IC<sub>50</sub> at nM levels, and cell survival at highest level on A549, NCI-H226, and CEM cell lines respectively at 28%, 17% and 0% for CEM

Knowing that cells can develop P-glycoprotein efflux pump mediated were resistant to colchicine were also conducted studies to determine that CCI-001 is a weak substrate for P-gp. Those studies suggested that P-gp might be a contributing factor to Cci-001 drug resistance, but many times less pronounced levels than colchicine [87]. The use of CCI-001 against bladder cancer line in T24-pretreated mice was assessed to be efficient, also in combination with other compounds cisplatin and CCI-001 plus gemcitabine resulting both highly synergistic. report report demonstrated the CCI-001 as a promising

new chemotherapeutic agent for cancer, active against many different types of cancer and highly effective against cancers that are resistant to standard therapies[88].

## **4 Aim of the work**

This thesis project aims to develop protocols for the production of polyurethane nanoparticle for the encapsulation of Colchicine derivatives, using both hydrophobic and hydrophilic drug analogues. For the hydrophilic formulation the method chosen is a slightly modified ionic gelation method with a hydrophilic proprietary polyurethane, a poly( $\epsilon$ -caprolactone) (PCL)/poly (ethylenglicol) (PEG) based PUR in a 50%(w/w) ratio, with PCL responsible of the core stability and PEG for the water solubility of the polymer, or chitosan. Polyelectrolyte complexation/ionic gelation is a simple method that uses very mild conditions, avoiding harmful organic solvents or high shear forces, therefore has capability to protect encapsulated molecules and to retain their activity after encapsulation. In addition, reversible physical crosslinking by electrostatic interaction instead of chemical crosslinking reduces the risk of toxicity. For the hydrophobic drug formulation, we adopted a core-shell nanoparticle structure produced by the nanoprecipitation/self-assembly method, using a hydrophobic polyesterurethane. We used a proprietary poly(caprolactone) (PCL)-based polyurethane for the polymeric core, and a mixture of lipids (DSPE-PEG and EGG-PG) for the lipidic shell. The nanoprecipitation is a relatively simple nanoparticle production method, in which nanoparticles are formed immediately without the use of intense mechanical efforts, in the absence of toxic solvents. The main purpose in encapsulating drugs with nanoparticles, is to avoid the most recurrent problems with the systemic chemotherapy, such as the side effects caused by the off target accumulation, exploiting the EPR effect, and also to preserve the drug integrity during its transport. The hydrophobic drug is CCI-001, also known as CR42-024, a promising novel agent, derivative from colchicine developed by the team of Prof. J. Tuszynski, a microtubule destabilizing agent that has showed its potentiality against several cancer cell lines. The work showed that nanoparticles could be obtained with both methods, having narrow size distribution. We also showed that the nanoprecipitation method favoured the encapsulation of the hydrophobic drug CCI-001, an anti-mitotic novel compound, developed to destabilize the microtubule polymerization and to improve the selectivity to  $\beta$ -III tubulin, the overexpression of which is associated with cancer activity. The un-encapsulated drug demonstrated strong cytotoxic activity against the U87MG cell line at nanomolar concentration, confirming the potentiality of the compound and encouraging further tests with the drug encapsulated in the nanoparticle formulation.

## **5 Materials and methods**

### **5.1 Materials**

#### **5.1.1 Chemicals and cell lines**

For nanoparticles (NPs) suitable for hydrophobic drug encapsulation, a proprietary poly-caprolactone (PCL)-based polyurethane (NS-HC2000) was used. The polymer

was synthesized using Poly( $\epsilon$ -caprolactone)-diol (2000 g/mol), nBOC Serinol as chain extender, Dibutyl Dilaurate (DBTL) as catalyst, and 1,6 Hexamethylene diisocyanate (HDI), all purchased from Sigma Aldrich (Italy). The lipid shell of the NPs is composed of a mixture of L- $\alpha$ -phosphatidylglycerol (EGG-PG) and 1,2-Distearoyl-sn-glycero-3-phosphoethanolaminePoly (ethylene glycol) (DSPE-PEG), both purchased from Avanti® Polar Lipids. All solvents were of analytical grade. For nanoparticles (NPs) for the encapsulation of water-soluble drugs, a proprietary poly-caprolactone (PCL)/poly-ethyleneglicol(PEG)based polyurethane (SHC2KE2K) was used. The polymer was synthesized using Poly(caprolactone)-diol (2000 g/mol), Poly(ethylen-glicol) (2000 g/mol), n-BOC Serinol as chain extender, Dibutyl Dilaurate (DBTL) as catalyst, and 1,6 Hexamethylene diisocyanate (HDI), and sodium tripolyphosphate (TPP). Encapsulated drug was CCI-001, a novel hydrophobic drug formulation, derived by thiocolchicine, developed by the Tuszynski team in the university of University of Alberta. Fluorescent NPs were obtained by adding a fluorophore, Rhodamine 123 purchased from Sigma Aldrich (Italy). For cell culture, we used a glioblastoma human cell line (U87 MG, American Type Culture Collection, ATCC®, HTB14™) in Gibco™ minimal essential medium (MEM) supplemented with 10% foetal bovine serum (FBS, Gibco™), and 1% penicillin/streptomycin (Gibco™). Cell viability was evaluated by using the CellTiter-Glo® 3D Cell Viability Assay (Promega).

## 5.2 Methods

### 5.2.1 Nanoparticles Preparation

#### Hydrophobic Nanoparticle formulation

NS-HC2000 was dissolved in acetonitrile (ACN) to produce a 10 mg/mL stock solution. The polymer was diluted to 1 mg/ml in 1 ml ACN and added dropwise to a solution of EGG-PG (200  $\mu$ g) and DSPE-PEG (240  $\mu$ g) in double-distilled water (ddH<sub>2</sub>O 2 mL). To obtain NPs, the lipid solution was maintained under stirring (250 rpm) at 60 °C to avoid the formation of micelles, followed by dropwise addition of the polymer solution in ACN to induce the spontaneous formation of nanoparticles. Finally, 1 mL of water was added drop-wise to promote temperature reduction and solvent evaporation. The particle suspension was centrifuged using Amicon® Ultra centrifugal filter units (equipped with a 10 kDa cutoff-membrane) for 13 min at 3200 rpm and room temperature (RT). The particles were resuspended in 1 mL of water for subsequent characterizations. For drug loaded NPs, 100  $\mu$ g of CCI-001 were added to the polymer solution in ACN. Figure 1 schematically summarizes the steps of NPs synthesis.

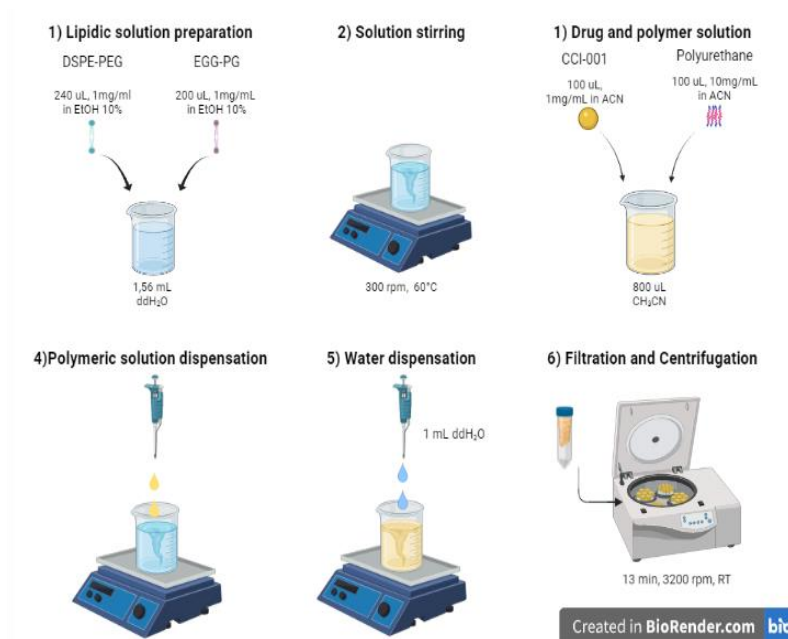


Figure 12:Hydrophobic NPs synthesis protocol loaded with CCI-0011

### Hydrophilic Nanoparticle formulation

SHC2KE2K was dissolved in Chloroform (CF) to produce a 100 mg/mL stock solution. 5 mg of polymer was then diluted into a 5ml CF/water solution, we started with different ratio(v/v) of CF and ddH<sub>2</sub>O at pH 5 in order to evaluate the optimal condition in terms of size and PDI of the nanoparticles. The three initial ratios of CF were: 50, 25, 10% of the 5ml solution, with the rest of the solution being water. To obtain NPs, the polymer solution was maintained under stirring (1250 rpm) at Room Temperature (RT) for 1 hour to allow CF to evaporate completely, obtaining a visually a transparent solution. Then, 0.5 mL of TPP solution in dH<sub>2</sub>O (2mg/ml) was added dropwise to the polymer solution reducing the stirring to 300 rpm and allowed to react for 30 minutes. Figure 2 schematically summarizes the steps of NPs synthesis. We also evaluated the efficacy of a 5 minutes of centrifugation at 3000rpm in the removal of aggregates of big particles and unreacted polymer, by picking out only the supernatant.

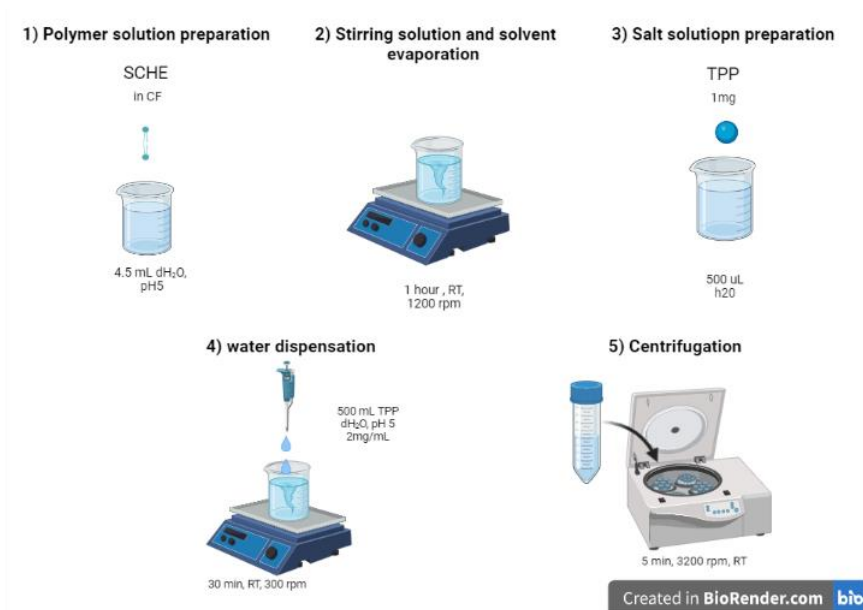


Figure 13:Hydrophilic nanoparticle preparation method

After this we tried another formulation with a 1% of CF and 99% of water (v/v), in order to reduce as much as possible the presence of CF. We also modified the molar ratio of TPP/PUR from 1:1 to 1:4 by adding 0.125 ml of the 2mg/ml TPP solution in ddH<sub>2</sub>O. We then evaluated PDI, size and zeta-potential of the nanoparticles. Based on the results from the optimization steps, the optimal protocol for PUR NP preparation with the ionic gelation method is described below:

SHC2KE2K was dissolved in Chloroform (CF) to produce a 100 mg/mL stock solution. 5 mg of polymer diluted into a 5ml solution of CF/ddH<sub>2</sub>O with a 10% of CF volume, the polymer solution was maintained under stirring (1250 rpm) at Room Temperature (RT) for 1 hour to allow CF to evaporate completely, obtaining a visually a transparent solution. Then, 0.5 mL of TPP solution in ddH<sub>2</sub>O (2mg/ml) was added dropwise to the polymer solution reducing the stirring to 300 rpm and let it react for 30 minutes. After that in order to remove eventual aggregates, the solution was centrifugated at 3000rpm for 5 minute, prelevating only the supernatant. After optimizing the NP solution, it was slightly modified as shown in Figure 3 to test the Rhodamine 123 encapsulation. 200,100,50,20 ug of Rh123 in 0.5 mg/ml solutions of Rh123/ddH<sub>2</sub>O was added after the complete evaporation of the CF and before the dropwise adding of the TPP/water solution. To eliminate the Rhodamine not encapsulated after the first centrifugation, the solution was filtrated four times in a 10 KDa cut-off filter at 3200 rpm.

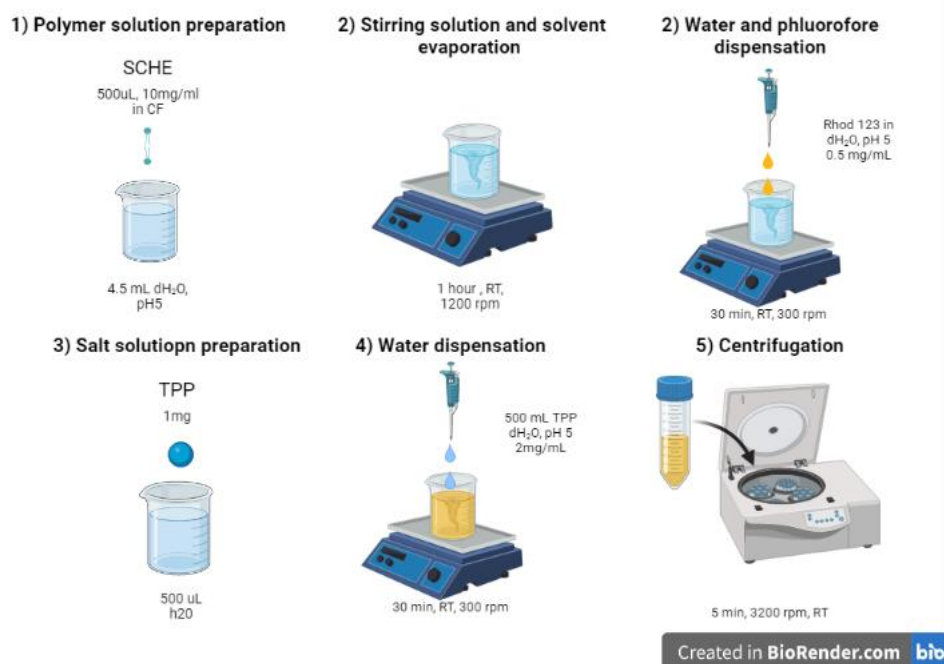


Figure 14: Hydrophilic NPs synthesis protocol with the phluorophore

### Nanoparticles characterization

NPs were analyzed through Dynamic Light Scattering (DLS) to derive the hydrodynamic diameter and polydispersity. Surface charge was also measured, using the dedicated Litesizer™Omega cuvettes (polycarbonate case with gold electrode). These physical characterizations were performed using a Litesizer™500 (Anton Paar). The evaluation of the hydrodynamic diameter is based on the empirical consideration that smaller particles move in suspension with a higher diffusion velocity. The instrument records over time the scattered light intensity after irradiating the NPs suspension with a He-Ne laser. The faster the particles move in solution, the greater the fluctuation of scatter intensities over time. The autocorrelation function is used to define the NPs diffusion coefficient, which is related to the average hydrodynamic diameter through the Stokes-Einstein equation. The hydrodynamic diameter does not represent the actual NPs size since it corresponds to the diameter of a hypothetical sphere that diffuses in solution with the same velocity as the particle of interest. The solution characteristics, the core size, NPs shape and surface properties strongly influence this parameter. DLS analysis returns a coefficient between 0 and 1 (called polydispersity index, PDI) that represents the uniformity of the diameter distribution. Hence, the smaller the PDI, the more the suspension is monodispersed. As above-mentioned, the zeta potential is evaluated using specific omega cuvettes equipped with gold electrodes to apply a voltage difference to the suspension of NPs. The migration velocity of the particles between the electrodes is proportional to the zeta potential, i.e. the charge of the layer between particle and ions dispersed in the medium. The zeta potential is an

index of the stability of the suspension. Therefore, the higher the absolute value (i.e. the net charge), the lower the risk of aggregation and the higher the suspension stability.

### **Drug encapsulation and release**

The encapsulation efficiency (%) was calculated for CCI-001-NPs and Rhodamine 123-NPs by using a UV/VIS spectrophotometer (Lambda 365, Perkin Elmer®, Waltham, MA, USA) at 384 nm for CCI-001 and 500 nm for Rh-123. Briefly, freeze-dried CCI-001NPs were dissolved in 0.2 mL ACN to induce drug release, after that tACN was evaporated and 0.2 mL of ethanol were added, to precipitate the polymer and solubilize the drug. IThe supernatant, containing only the drug, was then collected and the amount of drug was assessed through an empiric calibration curve. For the Rh-123 NPs, freeze-dried NPs were dissolved in 0.05 mL CF to induce NP breaking and RH-123 release, followed by CF evaporation. After this, 0.15 mL of ddH<sub>2</sub>O were added to dissolve the drug. the amount of drug present in the NPs was assessed through an empiric calibration curve. The encapsulation efficiency (EE) was then determined from these data using the formula:

$$EE(\%) = \frac{\text{Amount of drug or fluorophore in NPs}}{\text{Amount of drug or fluorophore supplied}}$$

*Equation 1: Encapsulation Efficiency*

where the amount of drug in NPs is the CCI-001 or Rhodamine mass detected through UV/VIS spectroscopy, while the amount of drug supplied is the CCI001 or Rhodamine mass dissolved in the synthesis solution (100 µg for each NPs formulation). For drug release, CCI-001-NPs were incubated at 37 °C in 1 mL ddH<sub>2</sub>O. The amount of drug released was measured at different timepoints: 1 h, 3 h, followed by daily assessment up to 7 days. After each timepoint, the NPs suspension was centrifuged (Beckman Coulter Allegra X 30) at 12000 rpm for 15 min to isolate the NPs. The release solution was collected and freeze dried, while NPs were resuspended in 1 mL of fresh ddH<sub>2</sub>O. The released drug was measured by adding 0.5 mL of ACN to the freeze-dried release solution, followed by drug detection by UV-Vis.

### **5.2.2 Cellular tests**

#### **Pharmacological treatment on 2D cell cultured**

After the incubation period, the cells were treated with free CCI-001 (1 nM, 10 nM, 50 nM, 100 nM, 500 nM). Controls (i.e., untreated cells) were included in the experiment. U87 cells were culture in 96-well plates (9.000 cells/well) for 24h before treatment and cell viability was assessed at two timepoints after the treatment: 24 and 48h. The cells were also retested with free CCI-001, encapsulate CCI-001 and empty NPs at the timepoint of 48h(1 nM, 5 nM, 10 nM, 20 nM, 50nm, 100nM). After 24 and 48

h of exposure to free drug, we evaluated the cell viability. Cell viability was assessed by the CellTiter-Glo® 3D Cell Viability Assay (Promega). This assay identifies the number of viable cells by quantifying the presence of adenosine triphosphate (ATP). The CellTiter-Glo® 3D Reagent contains a substrate (luciferin) and a lysis agent, which induce cell membrane rupture and ATP release. A thermostable luciferase (Ultra-Glo™ Recombinant Luciferase) acts on the substrate by consuming ATP and generates a luminescent signal, which is proportional to the amount of ATP released (indicator of cellular metabolic activity). To determine viability, 100 µL of CellTiter-Glo® 3D Reagent were added to the wells containing cells (in 100 µL). The plate was allowed to equilibrate at room temperature, shaken protected from light for 5 min at 460 rpm to induce cell lysis. The content of the wells was then transferred to a 96-well opaque white plate and briefly shaken until complete bubble removal. Finally, the luminescence signal of each well was analysed by plate reader. Cell viability was expressed as a percentage of the luminescence value determined for untreated controls. After the four-day incubation period the spheroids were treated with free CCI-001. Controls (i.e., untreated TS) were included in the experiment.

#### **Pharmacological treatment on 3D cell cultured**

Tumour spheroids were obtained in ultra-low attachment U bottom plates (Thermo Scientific™ Nunclon™ Sphera™ 96-Well, Nunclon Sphera Treated, U-Shaped-Bottom Microplate) with a monoculture of primary tumour cells (U87). Briefly, cells were plated at 4,000 cells/well and allowed to form spheroids for 4 days. After the spheroids formed, were treated with free CCI-001, free NPs, and CCI-001 encapsulated in the NPs (1 nM, 5 nM, 10 nM, 20 nM, 50 nM, 100 nM). Controls (i.e., untreated cells) were included in the experiment. After 24 and 48 h of exposure to free drug, NPs, and drug in NPs, we evaluated the cell viability. Cell viability was assessed by the CellTiter-Glo® 3D Cell Viability Assay (Promega).

## **6 Result and Discussion**

### **6.1 Nanoparticles Characterization**

Iontropic gelation method NPs

For the ionotropic gelation method first, we optimized the protocol to obtain NPs with small size, monodispersed size distribution and a nearly neutral zeta potential as expected from the method [cit]. The first two parameters analysed were the volume ratio of CF/water in the polymer solution, and the influence of centrifugation and subsequent pick up of the supernatant, to remove massive aggregates.

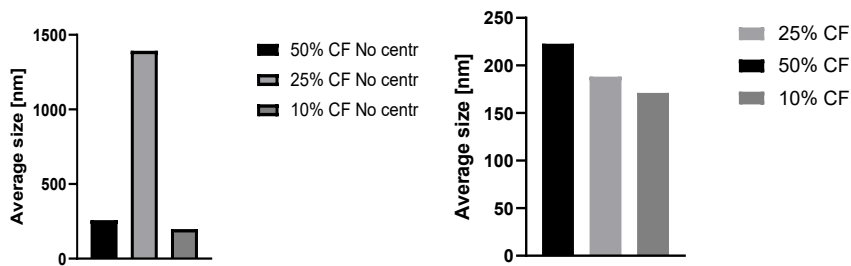


Figure 15: Size of NPs with 50,25 and 10% CF in the polymeric solution before and after centrifugation and picking up the supernatant.

Figure 2 shows the possibility to reduce the quantities of CF in the polymeric solution, reducing the NP size, except for the 25% of chloroform, were probably the size before centrifugation has some very big aggregation. The zeta-potential range goes from -3 mV to -3.9 mV, producing next to neutral NPs as expected. The centrifugation showed the ability to reduce the size of the NP and also the aggregates at 10  $\mu$ m as visible in the size distribution table

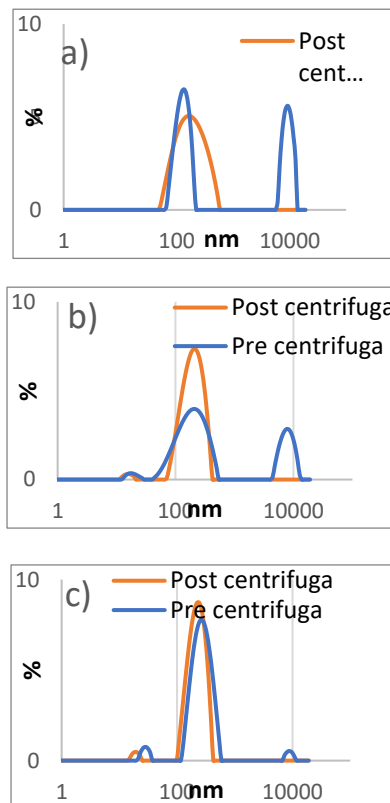


Figure 16: Size distribution for different CF percentage in the polymeric solution: a)50% CF formulation; b)25% CF formulation; c) 10 % CF formulation

Hence we opted to test for a further reduction of CF to 1% and comparing the results to the 10% condition. We analysed the PDI, zeta potential and PDI, this time analysing three sample for condition.

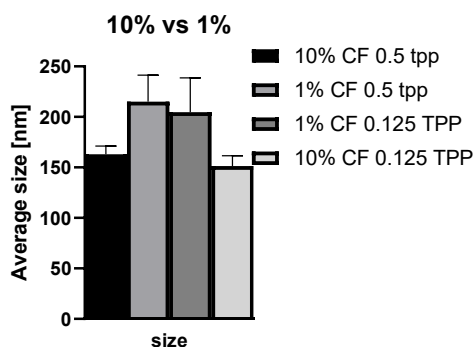


Figure 17: NPs size with 10% and 1% chloroform in polymer solution

The figure shows that 10% CF formulation produces smaller NPs with an average size under 200 nm, suitable for EPR effect, confirmed also by the unique peak in the size distribution, whereas the 1% CF formulation shows secondary peaks over 1µm, therefore. The PDI, instead remains quite the similar in the two formulations ranging from 24+3 to 27+2. Zeta potential instead changes with the TPP:PUR molar ratio from 14.1+0.5 with no TPP, to 2.2+0.9 with a 1:4 TPP:PUR molar ratio, to -4.7+1.7 to 1:1 molar ratio, showing changes of potential based on the TPP quantities, with statistical difference between all groups (p-value inferior to 0.05). All the values of z-potential are under the abs value of 20 mv, that could predict aggregation phenomena. So, the method for the rh123 encapsulation would be particle prepared in a solution with 10% of CF and a molar ratio of TPP:PUR 1:1. As showed in figure

#### Rhodamine 123 encapsulation

After the encapsulation of the Rh123 we analysed again PDI, zeta potential and size, and we also evaluated the encapsulation efficacy. After finding the empirical calibration curve we evaluated the encapsulation efficacy of Rh123 with various quantities: 200,100,50,20 µg in the NPs formulation with the result as in table 1.

Rhod supplied (ug)	EE (%)
200	0,75±0,16%
100	0,78±0,33%
50	1,60±0,54%
20	0,91±0,68%

Table 2: Encapsulation efficiency of Rhodamine 123

## 6.2 Hydrophobic NPs formulation

We evaluated size, PDI and zeta potential of NPs produced with nanoprecipitation method. The bare Nps resulted with small size. CCI-001 encapsulation resulted in a small increase in size in the 100ug formulation and a similar decrease for the 50 ug one. Empty and drug loaded NPs size are in the size range for EPR effects.

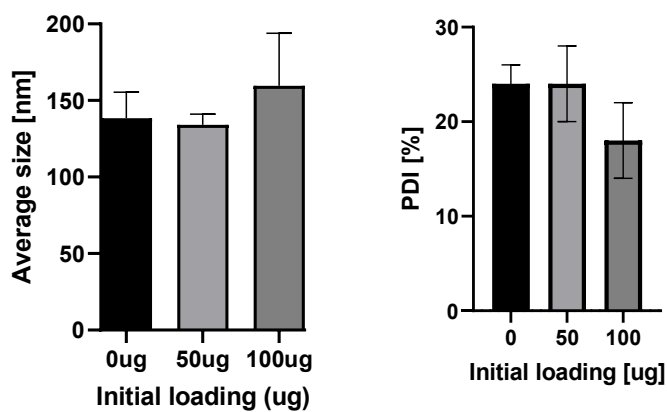


Figure 18:Hydrophobic NPs size with and without CCI-001 encapsulated

The size distribution resulted monodispersed as we can see in the size distribution graphs in figure 8.

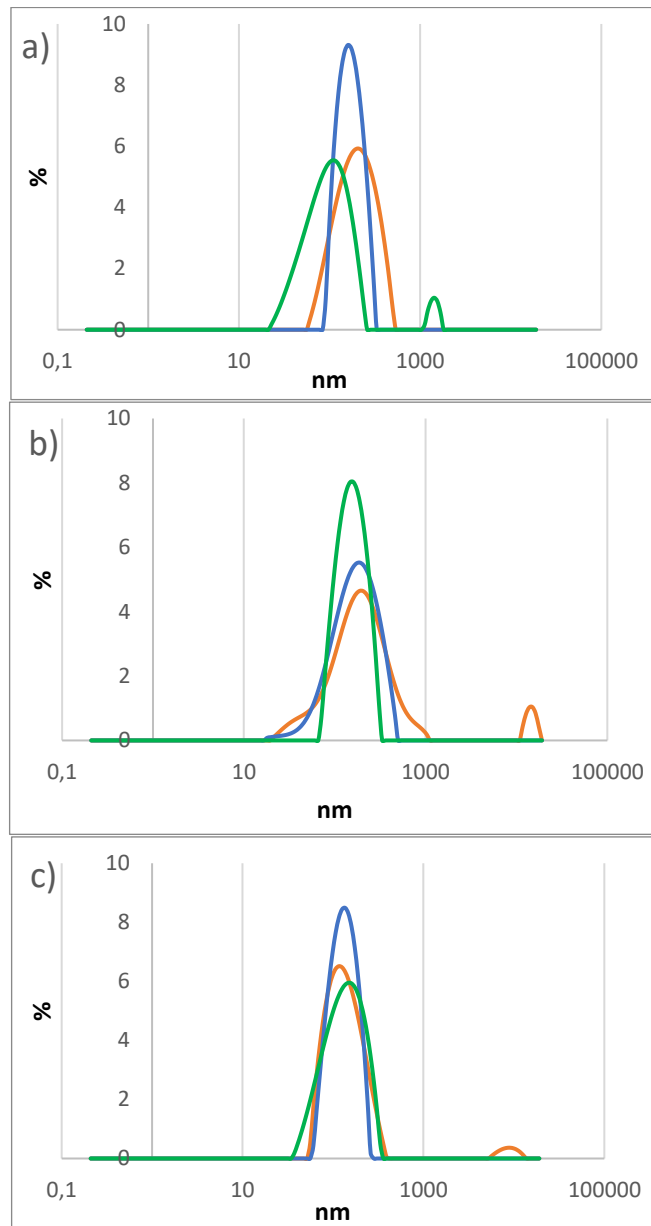


Figure 19: DLS Size distribution for n=3 samples of: a) empty NPs; b) NPs with 50ug of CCI-001 in formulation; c) NPs with 100ug of CCI-001 in formulation

### 6.3 Drug release

To evaluate release and EE we needed calibration curve in EtOH with the peak at 384 nm

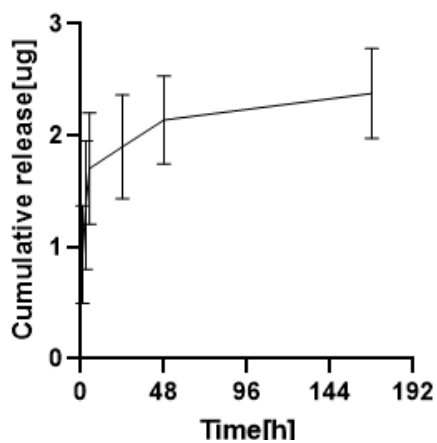


Figure 20: Release of CCI-001 in water

The release percentage was calculated on the percentage of the cumulative release results after 7 day showing a burst release in the first 24 hours of the 80% of drug released at 1 week

#### 6.4 Cellular tests

In figure is showed the morphology of U87 cells after the period of incubation

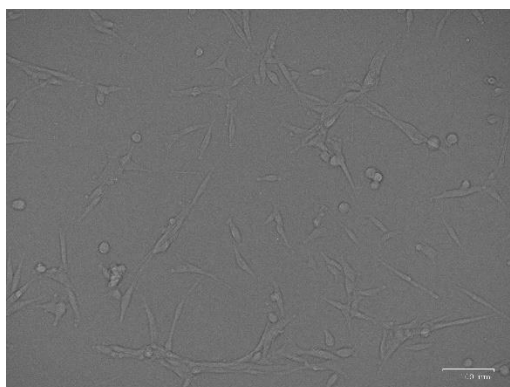


Figure 21: cultured U87 cells

### 6.4.1 Response of the cells to free CCI-001

The antitumor efficacy of free CCI-001 was analysed on u87 cells at two different timepoints: 24 and 48 hours with the result shown in figure

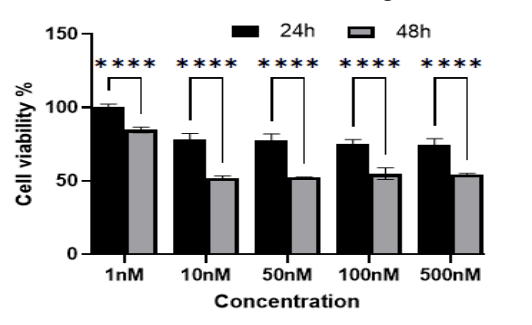


Figure 22: Cell viability of the cell exposed to free CCI-001 at various concentration at 24 and 48 h

Cell viability doesn't seem to be really affected by the concentration over 10 nM in much larger way even with the 500 nM, as there's no significant difference between the two concentration, whereas there is evidence that the 48h cell viability sample is more affected than the 24h.

After this we tested the same cell and compared the free drug effect on cell viability in comparison to empty NPs and encapsulated CCI-001 as shown in figure

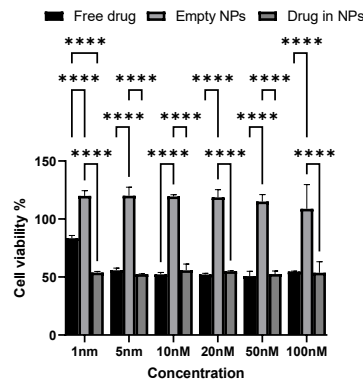
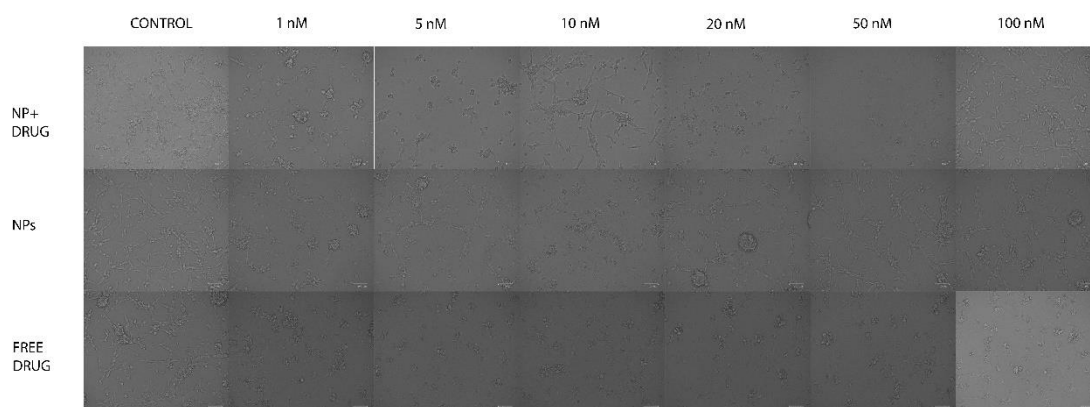


Figure 23: Cell viability 48 hours after exposure to different concentrations of free CCI-001, empty NPs and encapsulated CCI-001



*Figure 24: Images acquired in bright field microscopy for U87 cells treated with different concentration of free CCI-001, empty NPs and CCI-001 encapsulated in NPs observed at 48h*

As we can see in figure the empty NPs don't affect the cell viability at all, whereas the free and encapsulated CCI-001 seems to affect cell morphology from the concentration of 5 nM, with the exception of the 10 nM concentration of encapsulated drug that doesn't seem to affect the cell morphology.

#### 6.4.2 Tests on spheroids

Monocellular spheroids were successfully obtained as showed in figure

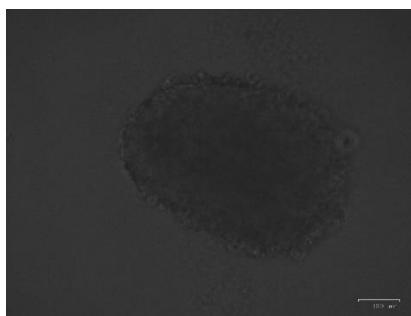


*Figure 25: U87 Cells spheroids after 4 days in culture*

The antitumor efficacy of free CCI-001, encapsulated CCI-001, and blank NPs was analysed on monocellular spheroids at two timepoints :24 and 48 hours. Regardless of the treatment considered, there are no significant morphological alterations in 48 hours as shown in figure

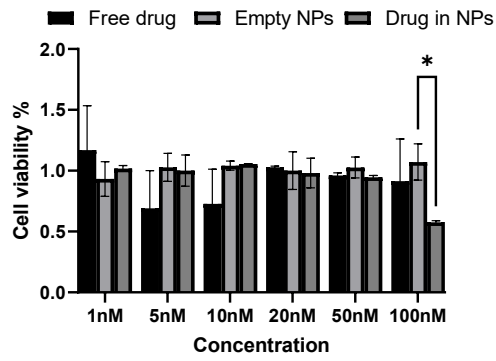


Figure 26: Cell viability of the spheroid treated with empty NPs, free CCI-001 and CCI-001 encapsulated in the NPs observed at 24 hours

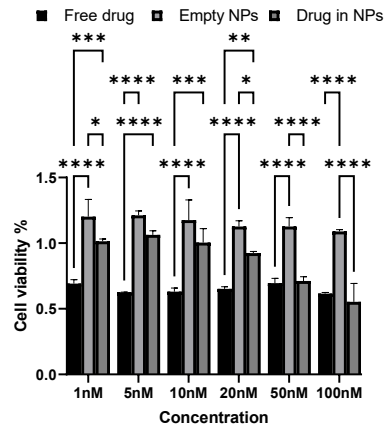


Figure 27: Cell viability of the spheroid treated with empty NPs, free CCI-001 and CCI-001 encapsulated in the NPs observed at 48 hours

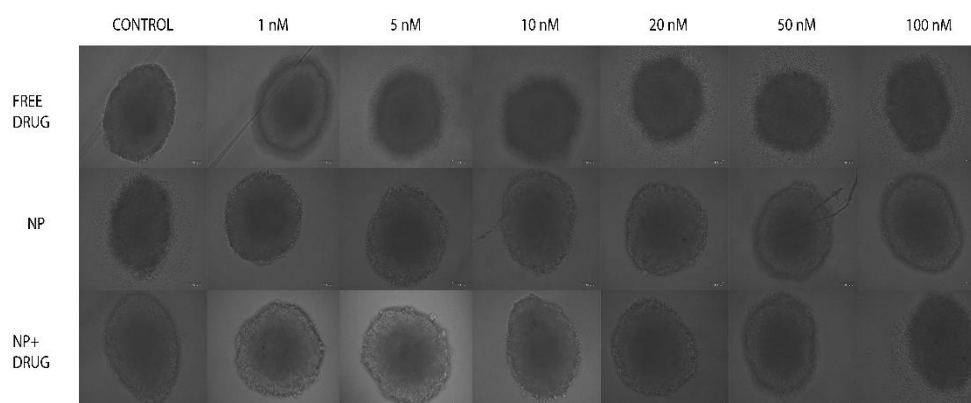


Figure 28: Images acquired in bright field microscopy for U87 spheroids treated with different concentration of free CCI-001, empty NPs and CCI-001 encapsulated in NPs observed at 48h

For the spheroids after 24 h the viability doesn't change significantly exposed to the drug encapsulated at lower concentration, instead at 100 nM the viability change drastically, with a better performance than free drug. After 48h hours the cell viability is more affected by the free drug at concentration range between 1 nM and 20 nM, at the two highest concentration the performance of the the free drug and encapsulated drug are similar. The empty NPs doesn't affect the viability of the cells, as expected from a biocompatible formulation. Morphologically there's no significant evidence of the diminished viability of the spheroids.

## 7 Conclusions

We successfully optimized the ionotropic gelation method to fit into the EPR effect range, with monodispersed size, suitable for hydrophilic compounds, next step could be to test different hydrophilic compounds and to test the Colchicine on cellular models in order to evaluate if the NPs formulation could reduce the side effects derived from the systemic subadministration, and if further functionalization of the NPs could enhance the specificity of this formulation towards the tumoral cells.

The Hydrophobic NPs formulation showed a good reproducibility, with size in the range of the EPR effect, and a good encapsulation efficiency towards this hydrophobic compounds, encouraging the trials with other hydrophobic drugs.

On the other hand the monocellular cell test of hydrophobic NPs formulation showed promising results in reducing glioblastoma cell viability, encouraging to analyse

more complex models of tumour introducing multicellular models that includes glioblastoma cells, to give more realistic results about the efficacy of the compound against glioblastoma related tumours, and analyse the possible drug resistance of more complex tumoral systems.

## 8 References

- [1] Paul Ehrlich. Beiträge zur theorie und praxis der histologischen färbung. In *The collected papers of Paul Ehrlich*, pages 29–64. Elsevier, 2013.
- [2] Richard Feynman. *There's plenty of room at the bottom*. CRC Press, 2018.
- [3] AC Anselmo and S Mitragotri. Nanoparticles in the clinic <https://doi.org/10.1002/btm2.10003> bioeng. transl, 2016.
- [4] Barenholz, Yechezkel Chezy. "Doxil®—the first FDA-approved nano-drug: lessons learned." *Journal of controlled release* 160.2 (2012): 117-134.
- [5] Wolfram, Joy / Ferrari, Mauro Clinical cancer nanomedicine 2019 Nano Today , Vol. 25 Elsevier p. 85-98
- [6] Mishra, Deepa, Justin R. Hubenak, and Anshu B. Mathur. "Nanoparticle systems as tools to improve drug delivery and therapeutic efficacy." *Journal of Biomedical Materials Research Part A: An Official Journal of The Society for Biomaterials, The Japanese Society for Biomaterials, and The Australian Society for Biomaterials and the Korean Society for Biomaterials* 101.12 (2013): 3646-3660.
- [7] Xu, Xiaoyang / Ho, William / Zhang, Xueqing / Bertrand, Nicolas / Farokhzad, Omid Cancer nanomedicine: from targeted delivery to combination therapy 2015 Trends in Molecular Medicine , Vol. 21, No. 4 p. 223-232
- [8] Singh, Rajesh, and James W. Lillard Jr. "Nanoparticle-based targeted drug delivery." *Experimental and molecular pathology* 86.3 (2009): 215-223.
- [9] Wang, Sheng, Peng Huang, and Xiaoyuan Chen. "Stimuli-responsive programmed specific targeting in nanomedicine." *Acs Nano* 10.3 (2016): 2991-2994.

- [10] Kobayashi, Hisataka, Rira Watanabe, and Peter L. Choyke. "Improving conventional enhanced permeability and retention (EPR) effects; what is the appropriate target?." *Theranostics* 4.1 (2014): 81
- [11] Yasuhiro Matsumura and Hiroshi Maeda. A new concept for macromolecular therapeutics in cancer chemotherapy: mechanism of tumoritropic accumulation of proteins and the antitumor agent smancs. *Cancer research*, 46(12 Part 1):6387–6392, 1986.
- [12] Swartz, M. A., & Lund, A. W. (2012). Lymphatic and interstitial flow in the tumour microenvironment: linking mechanobiology with immunity. *Nature Reviews Cancer*, 12(3), 210-219.
- [13] Remon Bazak, Mohamad Hourri, Samar El Achy, Serag Kamel, and Tamer Refaat. Cancer active targeting by nanoparticles: a comprehensive review of literature. *Journal of cancer research and clinical oncology*, 141(5):769– 784, 2015.
- [14] Bertrand, N., Wu, J., Xu, X., Kamaly, N., & Farokhzad, O. C. (2014). Cancer nanotechnology: the impact of passive and active targeting in the era of modern cancer biology. *Advanced drug delivery reviews*, 66, 2-25.
- [15] Ali, E. S., Sharker, S. M., Islam, M. T., Khan, I. N., Shaw, S., Rahman, M. A., ... & Mubarak, M. S. (2021, February). Targeting cancer cells with nanotherapeutics and nanodiagnostics: Current status and future perspectives. In *Seminars in cancer biology* (Vol. 69, pp. 52-68). Academic Press.
- [16] Anarjan, F. S. (2019). Active targeting drug delivery nanocarriers: Ligands. *Nano-Structures & Nano-Objects*, 19, 100370.
- [17] Marcucci, F., & Lefoulon, F. (2004). Active targeting with particulate drug carriers in tumor therapy: fundamentals and recent progress. *Drug discovery today*, 9(5), 219-228.
- [18] Rizzolo, Piera, et al. "Inherited and acquired alterations in development of breast cancer." *The application of clinical genetics* 4 (2011): 145.
- [19] Kale, A. A., & Torchilin, V. P. (2007). Design, synthesis, and characterization of pH-sensitive PEG– PE conjugates for stimuli-sensitive pharmaceutical nanocarriers: The effect of substitutes at the hydrazone linkage on the pH stability of PEG– PE conjugates. *Bioconjugate chemistry*, 18(2), 363-370.
- [20] van der Meel, R., Sulheim, E., Shi, Y., Kiessling, F., Mulder, W. J., & Lammers, T. (2019). Smart cancer nanomedicine. *Nature nanotechnology*, 14(11), 1007-1017.
- [21] Rao, N. Vijayakameswara, et al. "Recent progress and advances in stimuli-responsive polymers for cancer therapy." *Frontiers in bioengineering and biotechnology* (2018): 110.
- [22] S Lombardi Borgia, M Regehly, R Sivaramakrishnan, W Mehnert, HC Korting, K Danker, B Röder, KD Kramer, and M Schäfer-Korting. Lipid nanoparticles for skin penetration enhancement—correlation to drug localization within the particle

matrix as determined by fluorescence and piezoelectric spectroscopy. *Journal of controlled release*, 110(1):151–163, 2005.

- [23] MaLing Gou, ChangYang Gong, Juan Zhang, XiuHong Wang, XianHuo Wang, YingChun Gu, Gang Guo, LiJuan Chen, Feng Luo, Xia Zhao, et al. Polymeric matrix for drug delivery: Honokiol-loaded pcl-peg-pcl nanoparticles in peg-pcl-peg thermosensitive hydrogel. *Journal of Biomedical Materials Research Part A: An Official Journal of The Society for Biomaterials, The Japanese Society for Biomaterials, and The Australian Society for Biomaterials and the Korean Society for Biomaterials*, 93(1):219–226, 2010.
- [24] P Legrand, G Barratt, V Mosqueira, H Fessi, and J Ph Devissaguet. Polymeric nanocapsules as drug delivery systems. a review. *STP Pharma Sciences*, 9(5):411–418, 1999.
- [25] Muhammad Raza Shah, Muhammad Imran, and Shafi Ullah. *Lipid-based nanocarriers for drug delivery and diagnosis*. William Andrew, 2017.
- [26] Antonio Di Martino, Alena Pavelkova, Sandra Maciulyte, Saulute Budriene, and Vladimir Sedlarik. Polysaccharide-based nanocomplexes for co-encapsulation and controlled release of 5-fluorouracil and temozolomide. *European Journal of Pharmaceutical Sciences*, 92:276–286, 2016.
- [27] Hardman, Ron. "A toxicologic review of quantum dots: toxicity depends on physicochemical and environmental factors." *Environmental health perspectives* 114.2 (2006): 165-172.
- [28] Pouliquen, D., et al. "Iron oxide nanoparticles for use as an MRI contrast agent: pharmacokinetics and metabolism." *Magnetic resonance imaging* 9.3 (1991): 275-283
- [29] Espinosa, Ana, et al. "Magnetic (hyper) thermia or photothermia? Progressive comparison of iron oxide and gold nanoparticles heating in water, in cells, and in vivo." *Advanced Functional Materials* 28.37 (2018): 1803660.
- [30] Baino, Francesco, Sonia Fiorilli, and Chiara Vitale-Brovarone. "Bioactive glass-based materials with hierarchical porosity for medical applications: Review of recent advances." *Acta biomaterialia* 42 (2016): 18-32.
- [31] Prasad, Ram, et al. "Polymer based nanoparticles for drug delivery systems and cancer therapeutics." *Natural polymers for drug delivery*. Oxfordshire: CABI (2016): 53-70.
- [32] Yardley, D. A. (2013). nab-Paclitaxel mechanisms of action and delivery. *Journal of Controlled Release*, 170(3), 365-372.
- [33] Foland, T. B., Dentler, W. L., Suprenant, K. A., Gupta Jr, M. L., & Himes, R. H. (2005). Paclitaxel-induced microtubule stabilization causes mitotic block and apoptotic-like cell death in a paclitaxel-sensitive strain of *Saccharomyces cerevisiae*. *Yeast*, 22(12), 971-978.
- [34] Sur, S., Rathore, A., Dave, V., Reddy, K. R., Chouhan, R. S., & Sadhu, V. (2019). Recent developments in functionalized polymer nanoparticles for efficient drug delivery system. *Nano-Structures & Nano-Objects*, 20, 100397.

- [35] S Anju, N Prajitha, VS Sukanya, and PV Mohanan. Complicity of degradable polymers in health-care applications. *Materials Today Chemistry*,
- [36] u, Y., & Kao, W. J. (2010). Drug release kinetics and transport mechanisms of non-degradable and degradable polymeric delivery systems. *Expert opinion on drug delivery*, 7(4), 429–444. <https://doi.org/10.1517/17425241003602259>
- [37] Molavi, F., Barzegar-Jalali, M., & Hamishehkar, H. (2020). Polyester based polymeric nano and microparticles for pharmaceutical purposes: A review on formulation approaches. *Journal of Controlled Release*, 320, 265-282.
- [38] Ding, Xin, et al. "Antibacterial and antifouling catheter coatings using surface grafted PEG-b-cationic polycarbonate diblock copolymers." *Biomaterials* 33.28 (2012): 6593-6603.
- [39] Awasthi, V. D., et al. "Circulation and biodistribution profiles of long-circulating PEG-liposomes of various sizes in rabbits." *International journal of pharmaceutics* 253.1-2 (2003): 121-132.
- [40] Kawai, Fusako, and B. Schink. "The biochemistry of degradation of polyethers." *Critical reviews in biotechnology* 6.3 (1987): 273-307.
- [41] Wu D, Zhu L, Li Y, et al. Chitosan-based Colloidal Polyelectrolyte Complexes for Drug Delivery: A Review. *Carbohydr Polym.* 2020;238:116126. doi:10.1016/j.carbpol.2020.116126
- [42] Jiang, Hui, et al. "Conjugated polyelectrolytes: synthesis, photophysics, and applications." *Angewandte Chemie International Edition* 48.24 (2009): 4300-4316.
- [43] Mattu, Clara, et al. "Alternating block copolymer-based nanoparticles as tools to modulate the loading of multiple chemotherapeutics and imaging probes." *Acta biomaterialia* 80 (2018): 341-351.
- [44] Hu, K., Yuan, Y., Yan, P. *et al.* Green synthesis process and properties of polyurethane completely using ethanol as solvent. *J Polym Res* **24**, 80 (2017). <https://doi.org/10.1007/s10965-017-1240-5>
- [45] Kale, Santosh Nemichand, and Sharada Laxman Deore. "Emulsion micro emulsion and nano emulsion: a review." *Systematic Reviews in Pharmacy* 8.1 (2017): 39.
- [46] McCall, R. L., & Sirianni, R. W. (2013). PLGA nanoparticles formed by single-or double-emulsion with vitamin E-TPGS. *JoVE (Journal of Visualized Experiments)*, (82), e51015.
- [47] Bodmeier, R., J. Wang, and H. Bhagwatwar. "Process and formulation variables in the preparation of wax microparticles by a melt dispersion technique. II. W/O/W multiple emulsion technique for water-soluble drugs." *Journal of microencapsulation* 9.1 (1992): 99-107.
- [48] Abel, Silvestre Bongiovanni, et al. "Synthesis of polyaniline (PANI) and functionalized polyaniline (F-PANI) nanoparticles with controlled size by solvent displacement method. Application in fluorescence detection and bacteria killing by photothermal effect." *Nanotechnology* 29.12 (2018): 125604.

- [49] Mendoza-Muñoz, Néstor, David Quintanar-Guerrero, and Eric Allémann. "The impact of the salting-out technique on the preparation of colloidal particulate systems for pharmaceutical applications." *Recent Patents on Drug Delivery & Formulation* 6.3 (2012): 236-249.
- [50] Modena, Mario M., et al. "Nanoparticle characterization: what to measure?." *Advanced Materials* 31.32 (2019): 1901556.
- [51] Kumar, Ajeet, and Chandra Kumar Dixit. "Methods for characterization of nanoparticles." *Advances in nanomedicine for the delivery of therapeutic nucleic acids*. Woodhead Publishing, 2017. 43-58.
- [52] García, Mónica & Aloisio, Carolina. (2017). *Nanobiomaterials Nanostructured Materials for Biomedical Applications*.
- [53] Mohammed Yahaya Khan, Z. A. Abdul Karim, Ftwi Yohannes Hagos, A. Rashid A. Aziz, Isa M. Tan, "Current Trends in Water-in-Diesel Emulsion as a Fuel", *The Scientific World Journal*, vol. 2014, Article ID 527472, 15 pages, 2014. <https://doi.org/10.1155/2014/527472>
- [54] Wang, Yichao & Li, Puwang & Tran, Thao & Zhang, Juan & Kong, Lingxue. (2016). Manufacturing Techniques and Surface Engineering of Polymer Based Nanoparticles for Targeted Drug Delivery to Cancer. *Nanomaterials*. 6. 26. 10.3390/nano6020026.
- [55] Zielńska, Aleksandra & Carreiró, Filipa & Oliveira, Ana & Neves, Andreia & Pires, Bárbara & D., Nagasamy Venkatesh & Durazzo, Alessandra & Lucarini, Massimo & Eder, Piotr & Silva, Amélia & Santini, Antonello & Souto, Eliana B.. (2020). Polymeric Nanoparticles: Production, Characterization, Toxicology and Ecotoxicology. *Molecules*. 25. 3731. 10.3390/molecules25163731.
- [56] Geoffrey M Cooper and ROBERTE Hausman. A molecular approach. *The Cell. 2nd ed. Sunderland, MA: Sinauer Associates*, 2000.
- [57] Kendra S Burbank and Timothy J Mitchison. Microtubule dynamic instability. *Current Biology*, 16(14):R516–R517, 2006.
- [58] Gerhardt Attard, Alastair Greystoke, Stan Kaye, and Johann De Bono. Update on tubulin-binding agents. *Pathologie Biologie*, 54(2):72–84, 2006.
- [59] Elena Porcù, Roberta Bortolozzi, Giuseppe Basso, and Giampietro Viola. Recent advances in vascular disrupting agents in cancer therapy. *Future medicinal chemistry*, 6(13):1485–1498, 2014.
- [60] Frances Jane Sharom. Complex interplay between the p-glycoprotein multidrug efflux pump and the membrane: its role in modulating protein function. *Frontiers in oncology*, 4:41, 2014.
- [61] Cheol-Hee Choi. Abc transporters as multidrug resistance mechanisms and the development of chemosensitizers for their reversal. *Cancer cell international*, 5(1):1–13, 2005.
- [62] Young Hee Choi and Ai-Ming Yu. Abc transporters in multidrug resistance and pharmacokinetics, and strategies for drug development. *Current pharmaceutical design*, 20(5):793–807, 2014.

- [63] Wen Li, Han Zhang, Yehuda G Assaraf, Kun Zhao, Xiaojun Xu, Jinbing Xie, Dong-Hua Yang, and Zhe-Sheng Chen. Overcoming abc transporter-mediated multidrug resistance: Molecular mechanisms and novel therapeutic drug strategies. *Drug Resistance Updates*, 27:14–29, 2016.
- [64] Md Lutful Amin. P-glycoprotein inhibition for optimal drug delivery. *Drug target insights*, 7:DTI–S12519, 2013.
- [65] Kenneth D Tew. Glutathione-associated enzymes in anticancer drug resistance. *Cancer Research*, 76(1):7–9, 2016.
- [66] Ankita Bansal and M Celeste Simon. Glutathione metabolism in cancer progression and treatment resistance. *Journal of Cell Biology*, 217(7):2291–2298, 2018.
- [67] Ankush Prasad, Pavel Pospíšil, and Mika Tada. Reactive oxygen species (ros) detection methods in biological system. *Frontiers in physiology*, page 1316, 2019.
- [68] John D Hayes and Lesley I McLellan. Glutathione and glutathione-dependent enzymes represent a co-ordinately regulated defence against oxidative stress. *Free radical research*, 31(4):273–300, 1999.
- [69] Sehamuddin Galadari, Anees Rahman, Siraj Pallichankandy, and Faisal Thayyullathil. Reactive oxygen species and cancer paradox: to promote or to suppress? *Free Radical Biology and Medicine*, 104:144–164, 2017.
- [70] Kenneth H Downing and Eva Nogales. Tubulin and microtubule structure. *Current opinion in cell biology*, 10(1):16–22, 1998.
- [71] Luis J Leandro-García, Susanna Leskelä, Iñigo Landa, Cristina Montero-Conde, Elena López-Jiménez, Rocío Letón, Alberto Cascón, Mercedes Robledo, and Cristina Rodríguez-Antona. Tumoral and tissue-specific expression of the major human  $\beta$ -tubulin isoforms. *Cytoskeleton*, 67(4):214–223, 2010.
- [72] Luísa T Ferreira, Ana C Figueiredo, Bernardo Orr, Danilo Lopes, and Helder Maiato. Dissecting the role of the tubulin code in mitosis. In *Methods in cell biology*, volume 144, pages 33–74. Elsevier, 2018.
- [73] Lee-Chuan C Yeh, Asok Banerjee, Veena Prasad, Jack A Tuszynski, Alexander L Weis, Tamas Bakos, I-Tien Yeh, Richard F Ludueña, and John C Lee. Effect of ch-35, a novel anti-tumor colchicine analogue, on breast cancer cells overexpressing the  $\beta$ iii isotype of tubulin. *Investigational new drugs*, 34(1):129–137, 2016.
- [74] Marisa Mariani, Roshan Karki, Manuela Spennato, Deep Pandya, Shiquan He, Mirko Andreoli, Paul Fiedler, and Cristiano Ferlini. Class iii  $\beta$ -tubulin in normal and cancer tissues. *Gene*, 563(2):109–114, 2015.
- [75] Pascal Sève and Charles Dumontet. Is class iii  $\beta$ -tubulin a predictive factor in patients receiving tubulin-binding agents? *The lancet oncology*, 9(2):168–175, 2008.
- [76] Ying Ying Leung, Laura Li Yao Hui, and Virginia B Kraus. Colchicine— update on mechanisms of action and therapeutic uses. In *Seminars in arthritis and rheumatism*, volume 45, pages 341–350. Elsevier, 2015.

- [77] Baljinder Singh, Ashok Kumar, Prashant Joshi, Santosh K Guru, Suresh Kumar, Zahoor A Wani, Girish Mahajan, Aashiq Hussain, Asif Khurshid Qazi, Ajay Kumar, et al. Colchicine derivatives with potent anticancer activity and reduced p-glycoprotein induction liability. *Organic & biomolecular chemistry*, 13(20):5674–5689, 2015.
- [78] Jose M Andreu, Bernardo Perez-Ramirez, Marina J Gorbunoff, David Ayala, and Serge N Timasheff. Role of the colchicine ring a and its methoxy groups in the binding to tubulin and microtubule inhibition. *Biochemistry*, 37(23):8356–8368, 1998.
- [79] Jose Manuel Andreu and Serge N Timasheff. Conformational states of tubulin liganded to colchicine, tropolone methyl ether, and podophyllotoxin. *Biochemistry*, 21(25):6465–6476, 1982.
- [80] Manfred Roesner, Hans-Georg Capraro, Arthur E Jacobson, Louise Atwell, Arnold Brossi, Maria A Iorio, Thomas H Williams, Robert H Sik, and Colin F Chignell. Biological effects of modified colchicines. improved preparation of 2-demethylcolchicine, 3-demethylcolchicine, and (+)-colchicine and reassignment of the position of the double bond in dehydro-7deacetamidocolchicines. *Journal of medicinal chemistry*, 24(3):257–261, 1981.
- [81] Jing Chen, Tao Liu, Xiaowu Dong, and Yongzhou Hu. Recent development and sar analysis of colchicine binding site inhibitors. *Mini reviews in medicinal chemistry*, 9(10):1174–1190, 2009.
- [82] Anastasia Slobodnick, Binita Shah, Michael H Pillinger, and Svetlana Krasnokutsky. Colchicine: old and new. *The American journal of medicine*, 128(5):461–470, 2015.
- [83] Bhabatarak Bhattacharyya, Dulal Panda, Suvroma Gupta, and Mithu Banerjee. Anti-mitotic activity of colchicine and the structural basis for its interaction with tubulin. *Medicinal research reviews*, 28(1):155–183, 2008.
- [84] Monica S Charpentier, Rebecca A Whipple, Michele I Vitolo, Amanda E Boggs, Jana Slovic, Keyata N Thompson, Lekhana Bhandary, and Stuart S Martin. Curcumin targets breast cancer stem-like cells with microtentacles that persist in mammospheres and promote reattachment. *Cancer research*, 74(4):1250–1260, 2014.
- [85] B Gigant, A Cormier, A Dorléans, RBG Ravelli, and M Knossow. Microtubule-destabilizing agents: structural and mechanistic insights from the interaction of colchicine and vinblastine with tubulin. *Tubulin-Binding Agents*, pages 259–278, 2008.
- [86] Michael H Pillinger. Colchicine: Old and new. 2014.
- [87] Marc Christopher St George. *Drug Resistance in Breast Cancer: Characterization of Rationally Designed Paclitaxel Analogs in Model Systems*. University of Alberta (Canada), 2013.

[88] Clayton J Bell, Kyle G Potts, Mary M Hitt, Desmond Pink, Jack A Tuszynski, and John D Lewis. Novel colchicine derivative cr42-24 demonstrates potent anti-tumor activity in urothelial carcinoma. *Cancer letters*, 526:168– 179, 2022.